NACA

RESEARCH MEMORANDUM

LOW-SPEED WIND-TUNNEL INVESTIGATION OF LATERAL CONTROL CHARACTERISTICS OF A 60° TRIANGULAR-WING MODEL HAVING HALF-DELTA TIP CONTROLS

By Byron M. Jaquet and M. J. Queijo

Langley Aeronautical Laboratory
Langley Field, Va.

CLASSIFIED DOCUMENT

NATIONAL ADVISORY COMMITTEE
FOR AERONAUTICS

WASHINGTON

November 27, 1951

CONFIDENTIAL

Classification cancelled (or changed to Unclassified)

By Author's NASA Tech. Pub. Announcement

(OFFICER AUTHORIZED TO CHANGE)

By 18 Jan 64

(GRADE OF OFFICER MAKING CHANGE)

11 Feb 64

DATE

NATIONAL ADVISORY COMMITTEE FOR AERONAUTICS

RESEARCH MEMORANDUM

LOW-SPEED WIND-TUNNEL INVESTIGATION OF LATERAL CONTROL CHARACTERISTICS OF A 60° TRIANGULAR-WING MODEL HAVING HALF-DELTA TIP CONTROLS

By Byron M. Jaquet and M. J. Queijo

SUMMARY

A low-speed investigation was made in the Langley stability tunnel to determine the lateral control characteristics of a 60° triangular-wing model equipped with half-delta tip controls having areas of 5, 10, or 15 percent of the wing area (sum of left- and right-control areas).

The control effectiveness C_{l_δ} and rolling effectiveness $\frac{pb}{2V}/\delta$ of tip controls were found to be much lower than those for constant-chord controls of approximately the same area. The tip controls lost effectiveness with an increase in angle of attack much more rapidly than did the constant-chord controls. The control effectiveness and rolling effectiveness of tip controls increased in about direct proportion to the increase in control area at low angles of attack.

The control effectiveness and rolling effectiveness at moderate and high angles of attack could be improved by deflecting the controls symmetrically (trailing edge up) in conjunction with asymmetrical deflections. Symmetrical deflections in conjunction with asymmetrical deflections decreased the adverse yawing moments or made them favorable.

An available theory could be used with good accuracy to predict the control effectiveness and rolling effectiveness of half-delta tip controls at zero angle of attack.

INTRODUCTION

Several types of controls have been investigated on triangular wings, but the control aspects of these wings have not been as extensively investigated as have the aerodynamic characteristics (see, for example,

[redacted]

references 1, 2, and 3). Flap-type controls have good effectiveness at subsonic speeds but inherently have high hinge moments (references 4 and 5) along with a rapid loss in rolling effectiveness at transonic and supersonic speeds (reference 6). Half-delta tip controls permit a wide choice of hinge location to provide aerodynamic balance and have been found to have good rolling effectiveness at transonic and low-supersonic speeds (references 7 and 8).

In order to provide a more complete understanding of tip controls, a research program is being conducted in the Langley stability tunnel to determine the low-speed characteristics of these controls. Investigations have been made with a 60° triangular wing to determine the effects of symmetrical deflection of half-delta tip controls on the rolling characteristics of the wing (reference 9) and on the static longitudinal stability and control characteristics of the wing in combination with a fuselage (reference 10).

The present investigation presents the lateral control characteristics of a 60° triangular-wing model equipped with half-delta tip controls having areas of 5, 10, and 15 percent of the wing area (sum of left- and right-control areas). For a few tests, circular end plates were mounted on the wing adjacent to the inboard end of the 10-percent-area controls.

Although a specific theory for the control characteristics of triangular wings equipped with tip controls is lacking, the experimental data are compared with the theory of low-aspect-ratio wings of reference 11 where applicable.

SYMBOLS

The data presented herein are in the form of standard NACA symbols and coefficients of forces and moments which are referred to the stability system of axes with the origin at the projection of the quarter chord of the wing mean aerodynamic chord on the plane of symmetry. The positive directions of the forces, moments, and angular displacements are shown in figure 1. The symbols and coefficients used herein are defined as follows:

C_L lift coefficient $\left(\frac{L}{qS_w}\right)$

C_Y lateral-force coefficient $\left(\frac{Y}{qS_w}\right)$

C_m pitching-moment coefficient $\left(\frac{M}{qS_w\bar{c}}\right)$

C_n	yawing-moment coefficient $\left(\frac{N}{qS_w b}\right)$
C_l	rolling-moment coefficient $\left(\frac{L'}{qS_w b}\right)$
L	lift, pounds
Y	lateral force, pounds
M	pitching moment, foot-pounds
N	yawing moment, foot-pounds
L'	rolling moment, foot-pounds
A	wing aspect ratio $\left(\frac{b^2}{S_w}\right)$
b	wing span, feet
$\bar{c}$	wing mean aerodynamic chord, feet $\left(\frac{2}{S_w}\int_0^{b/2} c^2\,dy\right)$
c	wing local chord measured parallel to plane of symmetry, feet
S_w	wing area (including control area), square feet
S_c	control area (sum of left and right controls), square feet
y	spanwise distance measured from and perpendicular to plane of symmetry, feet
q	dynamic pressure, pounds per square foot $\left(\rho\frac{V^2}{2}\right)$
V	free-stream velocity, feet per second
α	angle of attack of fuselage center line, degrees
ρ	mass density of air, slugs per cubic foot
δ_{trim}	symmetrical deflection of left and right control surfaces from wing-chord plane, degrees
δ_R	deflection of right control with respect to wing-chord plane, degrees

[redacted]

δ total aileron deflection, degrees $\left(\delta_R - \delta_{trim}\right)$

$\frac{pb}{2V}$ wing-tip helix angle, radians

p rolling angular velocity, radians per second

$C_{Y_\delta} = \frac{\partial C_Y}{\partial \delta}$

$C_{n_\delta} = \frac{\partial C_n}{\partial \delta}$

$C_{l_\delta} = \frac{\partial C_l}{\partial \delta}$

$C_{l_p} = \frac{\partial C_l}{\partial \frac{pb}{2V}}$

$\frac{pb/2V}{\delta} = \frac{C_{l_\delta}}{C_{l_p}}$

Δ increment in control parameter caused by symmetrical control deflection δ_{trim}

APPARATUS, MODELS, AND TESTS

The present investigation was conducted in the 6- by 6-foot test section of the Langley stability tunnel with the model mounted on a single-strut support and pivoted about the quarter chord of the mean aerodynamic chord. The support strut was attached to a six-component balance system.

The model used in the present investigation was a wing-fuselage combination constructed primarily of laminated mahogany. The wing had a 60° sweptback leading edge, an aspect ratio of 2.31, a taper ratio of 0, and NACA $65_{(06)}$-006.5 airfoil sections parallel to plane of symmetry. The sections were modified by fairing straight lines from the 70-percent-chord line tangent to the trailing-edge radius. The trailing-edge angle was 8°. The fuselage had a circular cross section and a fineness ratio of 7.38 (fuselage ordinates may be obtained from reference 12). Pertinent model dimensions are given in figure 2.

The wing was equipped with half-delta tip controls having total areas (sum of left and right) of 5, 10, and 15 percent of the total

wing area. The hinge line of each control was at the center of the inboard chord of the control and was perpendicular to the plane of symmetry. Circular end plates, in the form of 10-inch disks of $\frac{1}{16}$-inch brass, were used with the 10-percent-area controls. The end plates were mounted adjacent to the inboard end of the tip controls with the gap between the control and end plate sealed for the tests. Photographs of the wing-fuselage combination having 10-percent-area tip controls without and with end plates are presented as figures 3(a) and 3(b), respectively.

The following table summarizes the tests of the present investigation:

δ_c/δ_w	δ_{trim} (deg)	δ_R (deg)	$\delta_R - \delta_{trim}$ (deg)	α (deg)
0.05, .10, .15	0	-30,-20,-10,0,10,20,30	-30,-20,-10,0,10,20,30	-4 to 36
	-10	-40,-30,-20,-10,0,10,20		
	-20	-50,-40,-30,-20,-10,0,10		
	-30	-60,-50,-40,-30,-20,-10,0		
.15	0	-8,-6,-4,-2,2,4,6,8	-8,-6,-4,-2,2,4,6,8	-4 to 12

The symbol δ_{trim} represents a symmetrical deflection of left and right controls. The tests with the 10-percent-area controls were made with and without end plates. The tests of the 15-percent-area controls at small deflections were made to determine the linearity of the forces and moments within the range used to determine the control parameters (10° to -10°).

All tests were made at a dynamic pressure of 39.7 pounds per square foot, a Mach number of 0.17, and a Reynolds number of 2.06×10^6 (based on the wing mean aerodynamic chord of 1.76 feet).

CORRECTIONS

Approximate corrections have been applied to the angle of attack to account for the effects of the jet boundaries. The methods of reference 13 were used to determine an approximate correction for the effects of blockage on the dynamic pressure. The data have not been corrected for the effects of the support-strut tares which are believed to be small. To account for slight model asymmetry, the values of C_Y, C_n, and C_l for $\delta_R - \delta_{trim} = 0°$ have been substracted from the data for other deflections.

[redacted]

[redacted]

RESULTS AND DISCUSSION

Preliminary Remarks

The longitudinal control characteristics of the model (obtained from reference 10) are presented in figure 4 to relate the lateral control characteristics of the model to the longitudinal trim conditions.

The basic lateral-control data (variation of C_Y, C_n, and C_l with α) presented in figures 5 to 8 were used to determine the control parameters C_{Y_δ}, C_{n_δ}, and C_{l_δ}. These parameters are slopes of curves of the coefficients measured between $\delta_R - \delta_{trim} = \pm 10^\circ$. In order to determine the linearity of the control parameters for control deflections smaller than those used to determine the slopes ($\delta_R - \delta_{trim} = \pm 10^\circ$), the 15-percent-area controls were deflected in 2° increments between $\delta_R - \delta_{trim} = \pm 8^\circ$. These data are presented in figure 9 in addition to data at other control deflections. Although the curves are nonlinear even for small control deflections, the slopes obtained by fairing the curves between ±10° are generally the same as those faired through $\delta_R - \delta_{trim} = 0^\circ$.

Lateral-Control Effectiveness

Effect of symmetrical control deflection.- The variation of C_{Y_δ}, C_{n_δ}, and C_{l_δ} with angle of attack for each model configuration and several trim conditions is presented in figure 10. For a given control size with $\delta_{trim} = 0^\circ$, as the angle of attack is increased the values of C_{Y_δ} and C_{n_δ} become more negative and more positive, respectively. The lateral-control effectiveness parameter C_{l_δ} generally decreases (becomes less negative) with an increase in angle of attack for each of the control sizes investigated with a reversal occurring at high angles of attack. The decrease in effectiveness with an increase in angle of attack can probably be attributed to the tip stall progressing inboard as the angle of attack is increased.

With respect to $\delta_{trim} = 0^\circ$ symmetrical control deflections ($\delta_{trim} = -10^\circ$, -20°, and -30°) generally made the values of C_{Y_δ} more positive and the values of C_{n_δ} more negative which results in a delay of the adverse yawing moments to higher angles of attack. At low angles of attack, small negative symmetrical control deflections generally have little effect on the control effectiveness C_{l_δ}, whereas large deflections generally cause a large decrease in C_{l_δ}. The investigation of reference 10

indicated that half-delta tip controls had low pitching-moment effectiveness and were effective as a trimming device only if the static margin at $C_L = 0$ was reduced considerably. Thus, it appears that symmetrical deflections would be used only as a means of delaying the tip stall to higher angles of attack. A large increase in control effectiveness can be obtained in the high angle-of-attack range if symmetrical negative deflections of -20° or less are used. Large negative deflections ($\delta_{trim} > -20^\circ$) generally do not provide an additional increase in control effectiveness at high angles of attack. The effects of symmetrical control deflection on the control characteristics of the 10-percent-area controls are shown in figure 11 in the form of ΔC_{Y_δ}, ΔC_{n_δ}, and ΔC_{l_δ}.

Effect of control area.- The data of figure 10 for symmetrical control deflections of 0° and -20° are replotted in figure 12 to show the effects of control area on the control parameters C_{Y_δ}, C_{n_δ}, and C_{l_δ}. The effects of control area on the control parameters are dependent to a large extent on the symmetrical control deflection. For $\delta_{trim} = 0^\circ$ (fig. 12(a)), an increase in control area causes an increase in control effectiveness $\left(C_{l_\delta}\right)$ up to angles of attack of about 16° but also increases the adverse yawing moments throughout the angle-of-attack range. The increase in control effectiveness is approximately proportional to the increase in control area for low angles of attack. Above angles of attack of 16° an increase in control area causes a positive increment in C_{l_δ}.

With $\delta_{trim} = -20^\circ$ (fig. 12(b)), the control effectiveness C_{l_δ} increases with an increase in control area up to angles of attack of about 32° and the yawing moments were favorable up to angles of attack of about 16°. At higher angles of attack, the yawing moments were adverse. Increasing the control area from 5 to 15 percent of the wing area made the yawing moments more favorable at angles of attack below 16° and made them more adverse at higher angles of attack. The curves of figure 13 show the angles of attack for which the yawing moment caused by control deflection was zero. The curves actually are boundaries of favorable and adverse yawing moments. The region below each curve has favorable yawing moments, whereas the region above had adverse yawing moments. Control area has little effect on the curves.

The control parameters C_{Y_δ}, C_{n_δ}, and C_{l_δ} of the 15-percent-area half-delta tip controls are compared with the control parameters of 16.3-percent-area constant-chord controls in figure 14 for $\delta_{trim} = 0^\circ$. The constant-chord controls are considerably better than the half-delta tip controls from the standpoint of both greater control effectiveness and generally smaller adverse yawing moments. The constant-chord controls do not lose control effectiveness with an increase in angle of attack as rapidly as do the tip controls.

[redacted]

Effect of end plates.- The effects of the addition of circular end plates adjacent to the inboard end of the 10-percent-area controls on the control parameters depend to some extent on the symmetrical control deflection and angle of attack (see figs. 10(b), 10(d), and 12). Generally the only consistent effect of the end plates was the increase in the values of C_{Y_δ} and C_{n_δ} at high angles of attack. The end plates generally had a detrimental effect on the control effectiveness through the angle-of-attack range except for $\delta_{trim} = -30^\circ$ at high angles of attack where the end plates increased the control effectiveness. The end plates delay the angle of attack for adverse yawing moments to higher angles of attack for symmetrical control deflections less than about -28° (fig. 13).

Rolling Effectiveness

Effect of symmetrical control deflection.- The rolling effectiveness parameter $\frac{pb}{2V}/\delta$ was obtained for each control configuration by use of the control effectiveness data C_{l_δ} of figure 10 and the damping-in-roll data (C_{l_p}) of reference 9. The effects of symmetrical control deflection on the rolling effectiveness parameter $\frac{pb}{2V}/\delta$ are shown in figure 15. The investigation of reference 9 indicated that the effects of symmetrical control deflection and control area on the damping in roll C_{l_p} were small.

With $\delta_{trim} = 0^\circ$ (fig. 15(a)), the maximum rolling effectiveness occurs at $\alpha = 0^\circ$ with a rapid loss in effectiveness occurring with an increase in angle of attack. This loss in rolling effectiveness can be attributed to the loss in control effectiveness with an increase in angle of attack (fig. 10). The primary effect of increasing the symmetrical control deflection is a reduction in the loss of rolling effectiveness which occurs with an increase in angle of attack. However, symmetrical control deflections do not increase the rolling effectiveness over that for $\alpha = 0^\circ$ and $\delta_{trim} = 0^\circ$. The constant-chord controls have greater rolling effectiveness (especially at high angles of attack) than the tip controls (fig. 15(a)).

Inasmuch as symmetrical control deflections improved the rolling effectiveness at moderate and high angles of attack, figure 16 was prepared to indicate the variation of $\frac{pb}{2V}/\delta$ with angle of attack when the controls were deflected symmetrically in direct proportion to the angle of attack beginning at $\alpha = 0^\circ$.

The data of figure 16 present the effects of variations in the rate of change of symmetrical control deflection with angle of attack $\frac{\partial \delta_{trim}}{\partial \alpha}$ on $\frac{pb}{2V}/\delta$ for each of the control sizes investigated. An increase in $\frac{\partial \delta_{trim}}{\partial \alpha}$ from 0 to -0.5 generally causes an increase in rolling effectiveness throughout the angle-of-attack range and delays the reversal that occurs at moderately high angles of attack to angles of attack above that for maximum lift (about $\alpha = 32^\circ$). When $\frac{\partial \delta_{trim}}{\partial \alpha}$ is equal and opposite to the angle of attack $\left(\frac{\partial \delta_{trim}}{\partial \alpha} = -1.0\right)$, an increase in rolling effectiveness is obtained throughout the angle-of-attack range only for the 15-percent-area controls (fig. 16(c)).

Effects of control area.- The effects of control area on $\frac{pb}{2V}/\delta$ are shown in figure 15 for several symmetrical control deflections. Inasmuch as control area and symmetrical control deflections had only small effects on C_{l_p} (reference 9), the effects of control area on $\frac{pb}{2V}/\delta$ are very nearly the same as the effects of control area on C_{l_δ}. For example, the data of figure 16, for $\frac{\partial \delta_{trim}}{\partial \alpha} = 0$ to -1.0 at low angles of attack, show that the rolling effectiveness increases about proportionally to the increase in control area. At high angles of attack, the effects of control area depend on the value of $\frac{\partial \delta_{trim}}{\partial \alpha}$.

Comparison of Control and Rolling Effectiveness with Theory

The dashed curves of figure 17 represent theoretical values of C_{l_δ}, $\frac{pb}{2V}/\delta$, and $\frac{pb/2V}{\delta}\frac{S_w}{S_c}$ for tip controls and were obtained from reference 11 for $\alpha = 0^\circ$ and $\delta_{trim} = 0^\circ$. The expression $\frac{pb/2V}{\delta}\frac{S_w}{S_c}$ can be considered as an efficiency factor since its use enables comparison on the same basis. As previously noted, the values of C_{l_δ} and $\frac{pb}{2V}/\delta$ increased with an increase in control area at low angles of attack. The values of C_{l_δ} and $\frac{pb}{2V}/\delta$ obtained from reference 11 are in very good agreement with the experimental values for $\frac{S_c}{S_w} = 0.05$. As the control area is increased, the theory tends to underestimate the effects of control area.

[redacted]

In terms of $\frac{pb/2V}{\delta}\frac{S_w}{S_c}$, the 5-percent-area tip controls are almost as efficient as the 16.3-percent-area constant-chord controls. The efficiency of the tip controls decreases with an increase in control area which is also indicated by the theory of reference 11.

CONCLUSIONS

The results of a low-speed investigation made in the Langley stability tunnel to determine the lateral control characteristics of a 60° triangular-wing model having half-delta tip controls have indicated the following conclusions:

1. The control effectiveness C_{l_δ} and rolling effectiveness $\frac{pb}{2V}/\delta$ of half-delta tip controls were much lower than those for constant-chord controls of approximately the same area. The tip controls also lost effectiveness much more rapidly with an increase in angle of attack than did the constant-chord controls.

2. The control effectiveness and rolling effectiveness of tip controls increased in about direct proportion to the increase in control area at low angles of attack.

3. The control effectiveness and rolling effectiveness at moderate and high angles of attack could be improved by deflecting the controls symmetrically (trailing edge up) in conjunction with asymetrical deflections. Symmetrical deflections in conjunction with asymmetrical deflections decreased or made favorable the adverse yawing moments.

4. An available theory could be used with good accuracy to predict the control effectiveness and rolling effectiveness at zero angle of attack.

Langley Aeronautical Laboratory
National Advisory Committee for Aeronautics
Langley Field, Va.

REFERENCES

1. Anderson, Adrien E.: An Investigation at Low Speed of a Large-Scale Triangular Wing of Aspect Ratio Two.- I. Characteristics of a Wing Having a Double-Wedge Airfoil Section with Maximum Thickness at 20-Percent Chord. NACA RM A7F06, 1947.

2. Jaquet, Byron M., and Brewer, Jack D.: Low-Speed Static-Stability and Rolling Characteristics of Low-Aspect-Ratio Wings of Triangular and Modified Triangular Plan Forms. NACA RM L8I29, 1949.

3. Brown, Clinton E., and Heinke, Harry S., Jr.: Preliminary Wind-Tunnel Tests of Triangular and Rectangular Wings in Steady Roll at Mach Numbers of 1.62 and 1.92. NACA RM L8L30, 1949.

4. Wolhart, Walter D., and Michael, William H., Jr.: Wind-Tunnel Investigation of the Low-Speed Longitudinal and Lateral Control Characteristics of a Triangular-Wing Model of Aspect Ratio 2.31 Having Constant-Chord Control Surfaces. NACA RM L50G17, 1950.

5. Stephenson, Jack D., and Ameudo, Arthur R.: Tests of a Triangular Wing of Aspect Ratio 2 in the Ames 12-Foot Pressure Wind Tunnel. II - The Effectiveness and Hinge Moments of a Constant-Chord Plain Flap. NACA RM A8E03, 1948.

6. Sandahl, Carl A.: Free-Flight Investigation of the Rolling Effectiveness of Several Delta Wing-Aileron Configurations at Transonic and Supersonic Speeds. NACA RM L8D16, 1948.

7. Sandahl, Carl A., and Strass, E. Kurt: Comparative Tests of the Rolling Effectiveness of Constant-Chord, Full-Delta, and Half-Delta Ailerons on Delta Wings at Transonic and Supersonic Speeds. NACA RM L9J26, 1949.

8. Martz, C. William, and Church, James D.: Flight Investigation at Subsonic, Transonic, and Supersonic Velocities of the Hinge-Moment Characteristics, Lateral-Control Effectiveness, and Wing Damping in Roll of a 60° Sweptback Delta Wing with Half-Delta Tip Ailerons. NACA RM L51G18, 1951.

9. Wolhart, Walter D.: Wind-Tunnel Investigation at Low Speed of the Effects of Symmetrical Deflection of Half-Delta Tip Controls of the Damping in Roll and Yawing Moment Due to Rolling of a Triangular-Wing Model. NACA RM L51B09, 1951.

[redacted]

10. Jaquet, Byron M., Queijo, M. J., and Lichtenstein, Jacob H.: Low-Speed Static Longitudinal Stability and Control Characteristics of a 60° Triangular-Wing Model Having Half-Delta Tip Controls. NACA RM L51D20a, 1951.

11. DeYoung, John: Theoretical Antisymmetric Span Loading for Wings of Arbitrary Plan Form at Subsonic Speeds. NACA TN 2140, 1950.

12. Jaquet, Byron M., and Brewer, Jack D.: Effects of Various Outboard and Central Fins on Low-Speed Static-Stability and Rolling Characteristics of a Triangular-Wing Model. NACA RM L9E18, 1949.

13. Herriot, John G.: Blockage Corrections for Three-Dimensional-Flow Closed-Throat Wind Tunnels, with Consideration of the Effects of Compressibility. NACA Rep. 995, 1950. (Formerly NACA RM A7B28.)

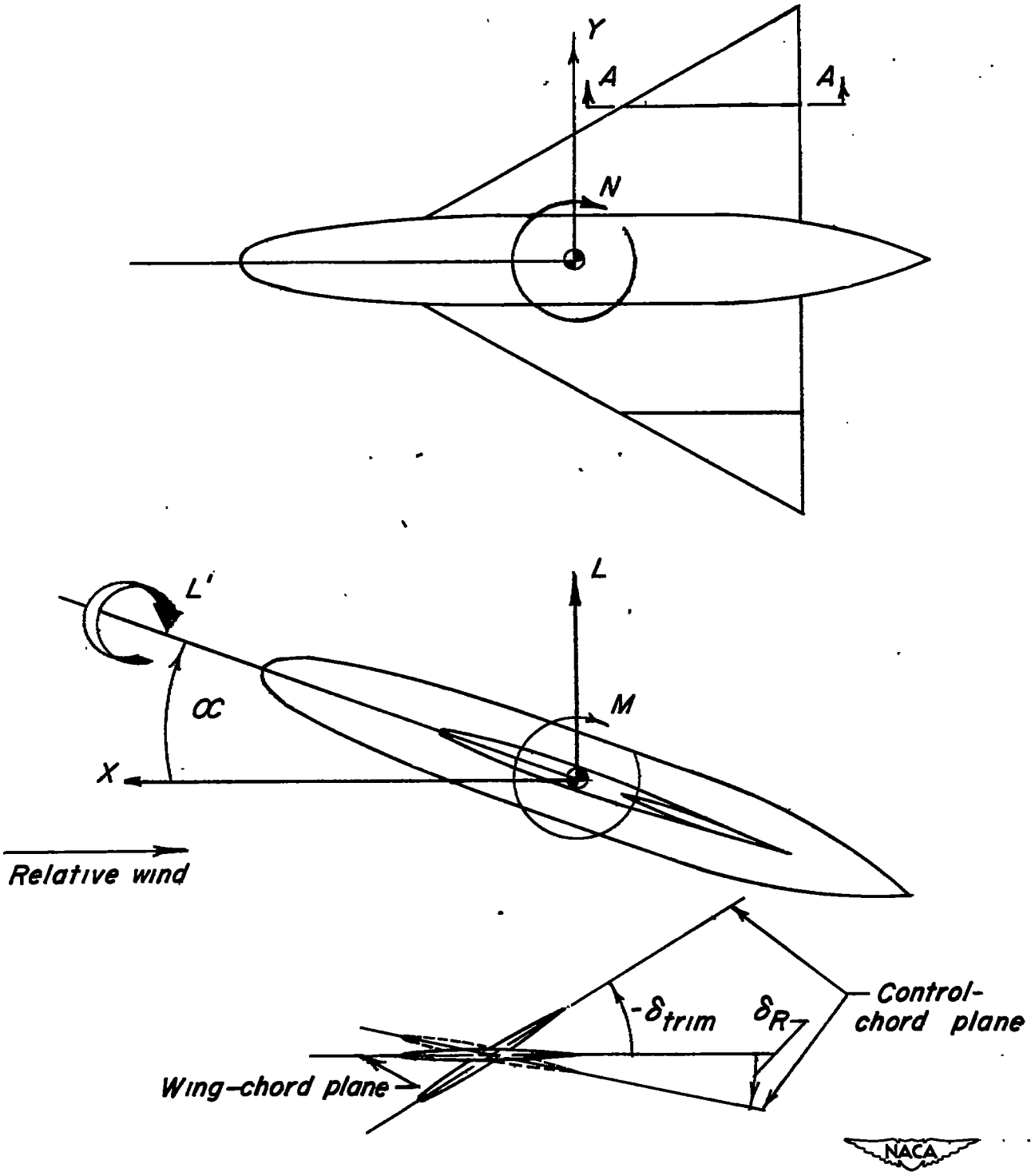

View A-A

Figure 1.- Stability system of axes. Arrows indicate positive direction of forces, moments, and angular displacements. Note exception for $-\delta_{trim}$.

[redacted]

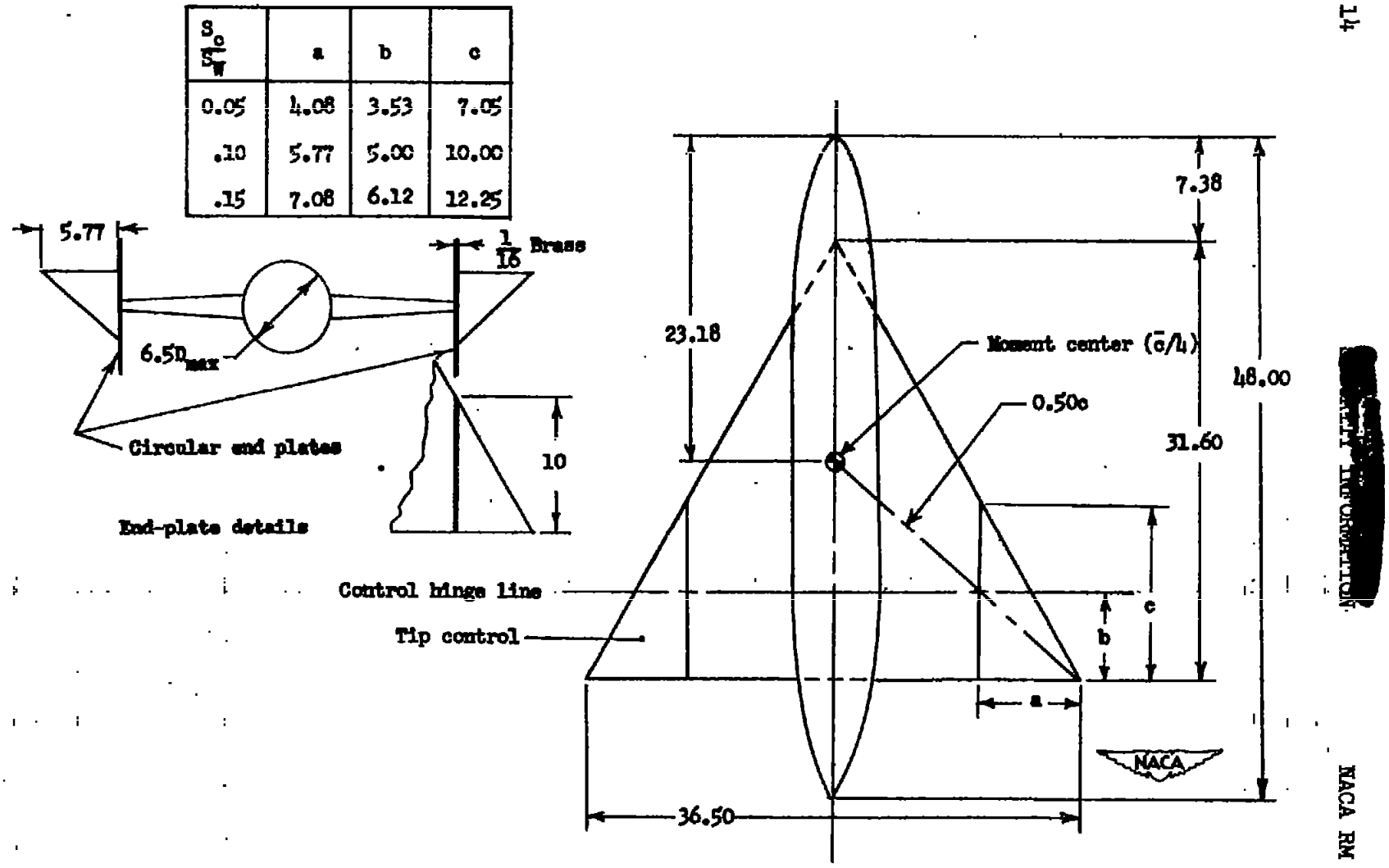

$\frac{S_c}{S_w}$	a	b	c
0.05	4.08	3.53	7.05
.10	5.77	5.00	10.00
.15	7.08	6.12	12.25

Figure 2.- Sketch of the model used in the investigation. (All dimensions are in inches.)

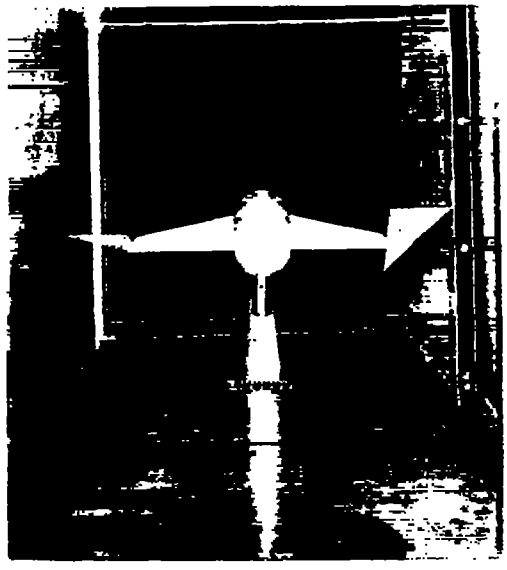

NACA L-68797

(a) Without end plates.

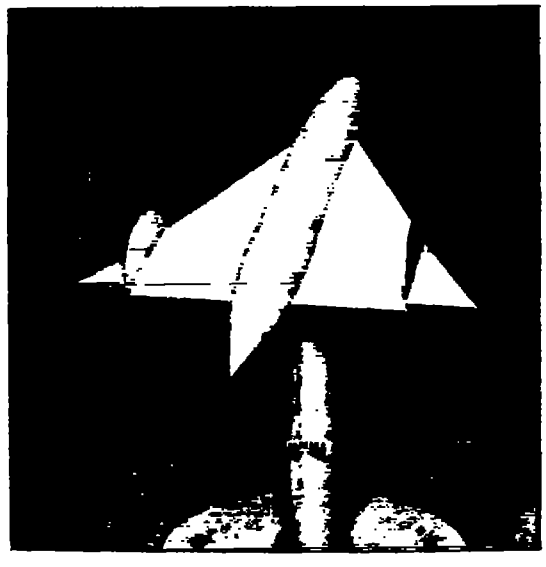

NACA L-67430

(b) With 10-inch diameter end plates.

Figure 3.- Model without and with end plates mounted in 6- by 6-foot test section of Langley stability tunnel. $\frac{S_c}{S_w} = 0.10$.

[redacted]

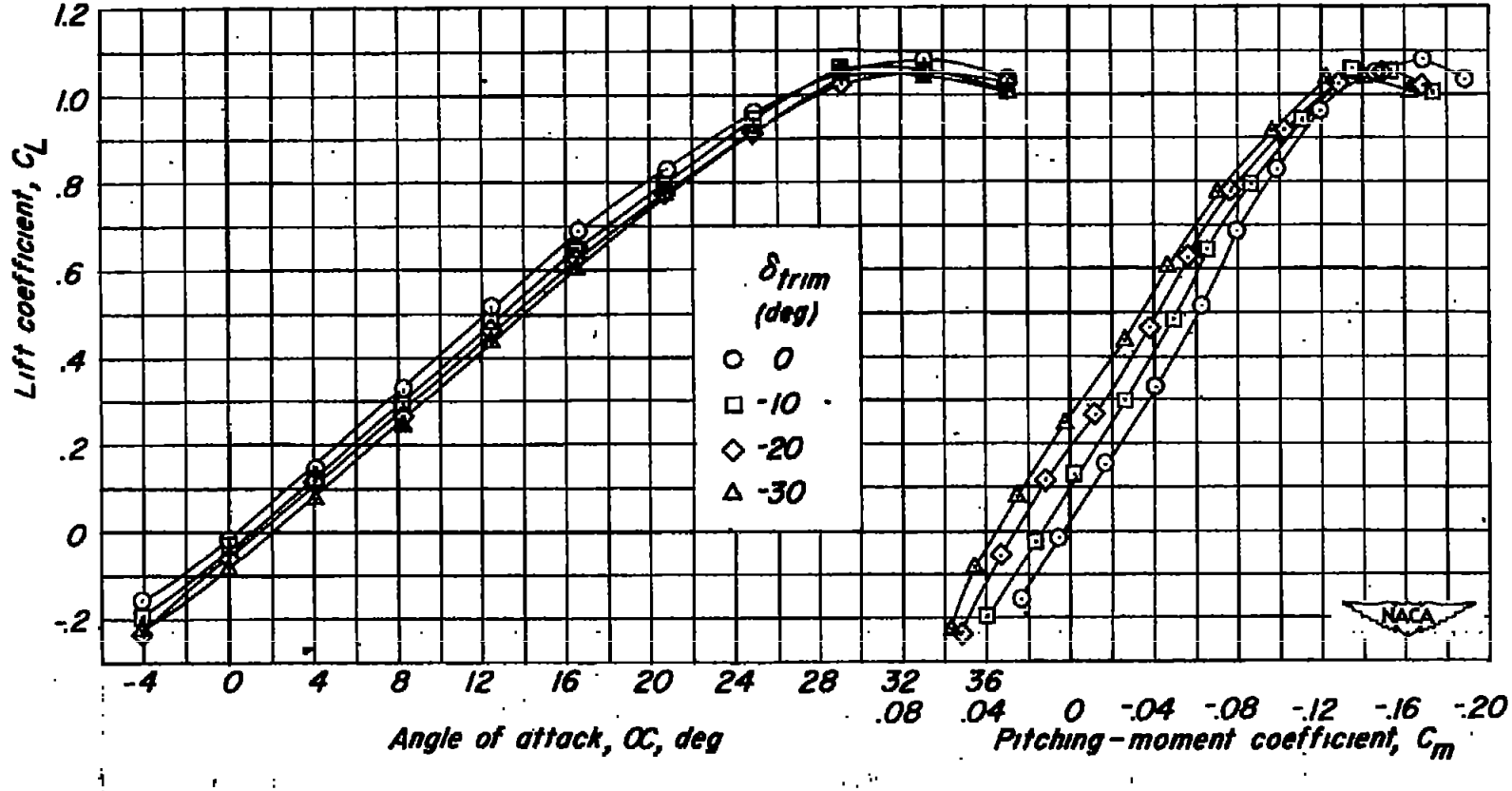

(a) $\frac{S_c}{S_w} = 0.05$.

Figure 4.- Longitudinal stability and control characteristics of a 60° triangular-wing model having half-delta tip controls. Data obtained from reference 10.

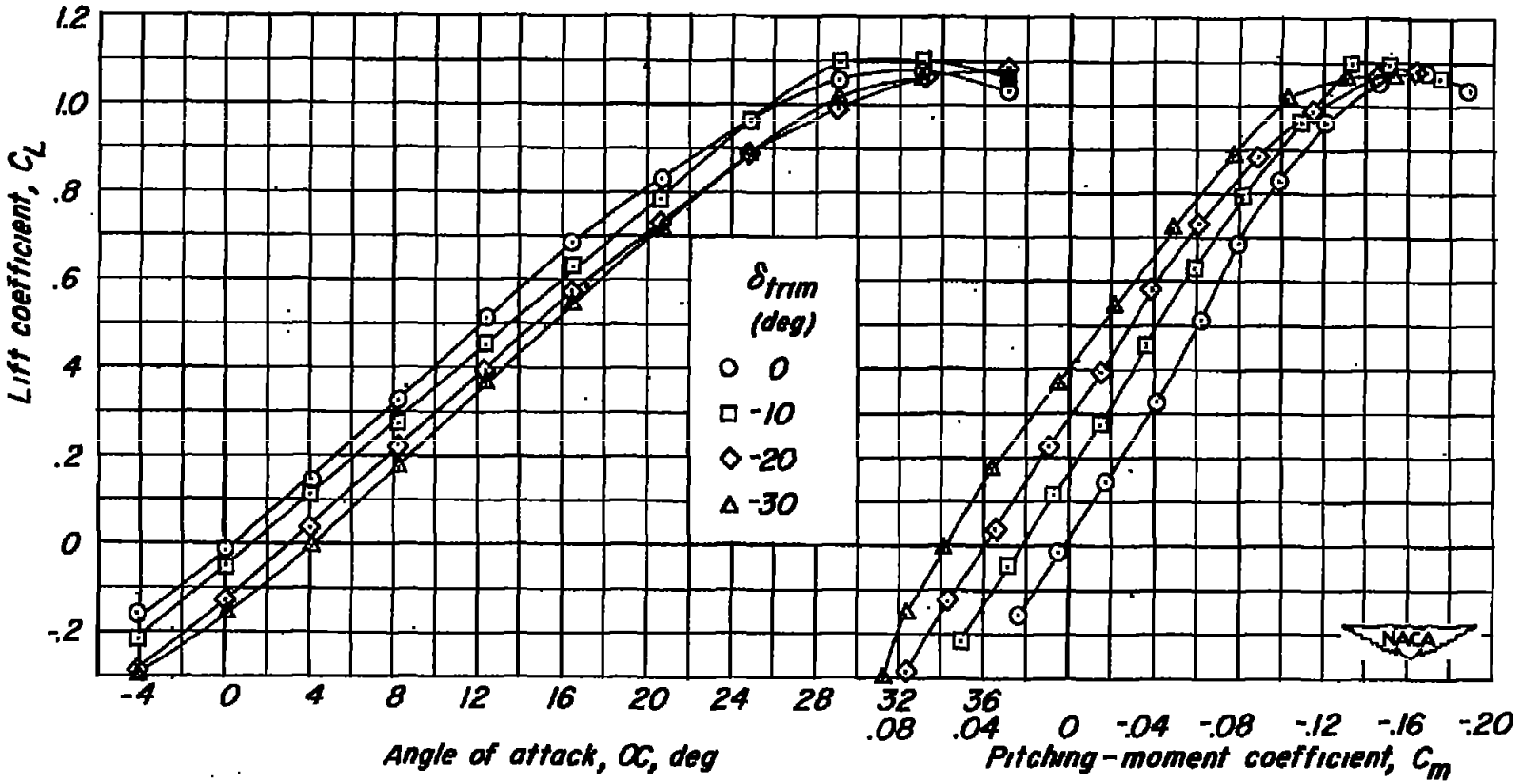

(b) $\frac{S_c}{S_w} = 0.10$.

Figure 4.- Continued.

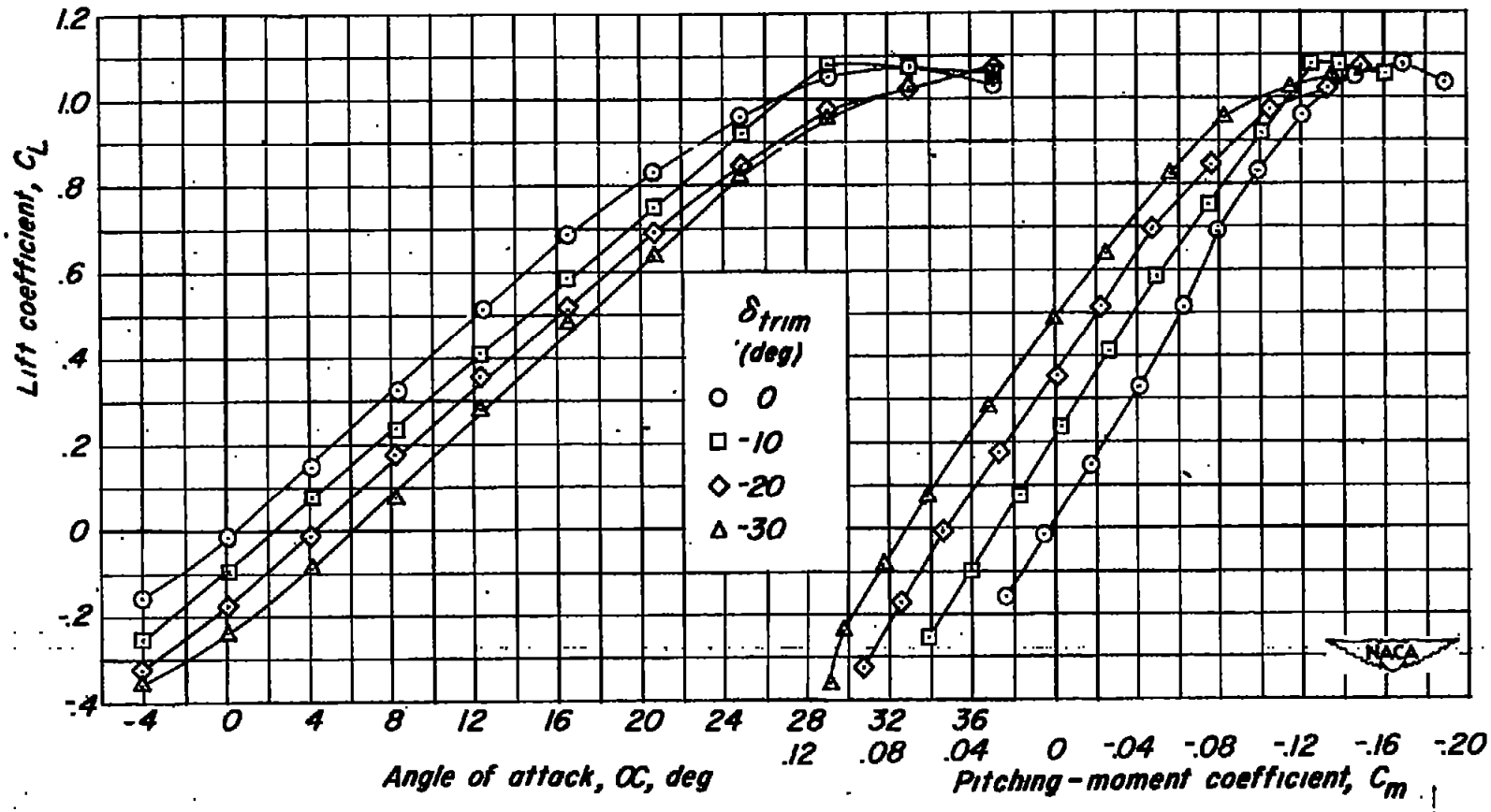

(c) $\frac{S_c}{S_w} = 0.15$.

Figure 4.- Continued.

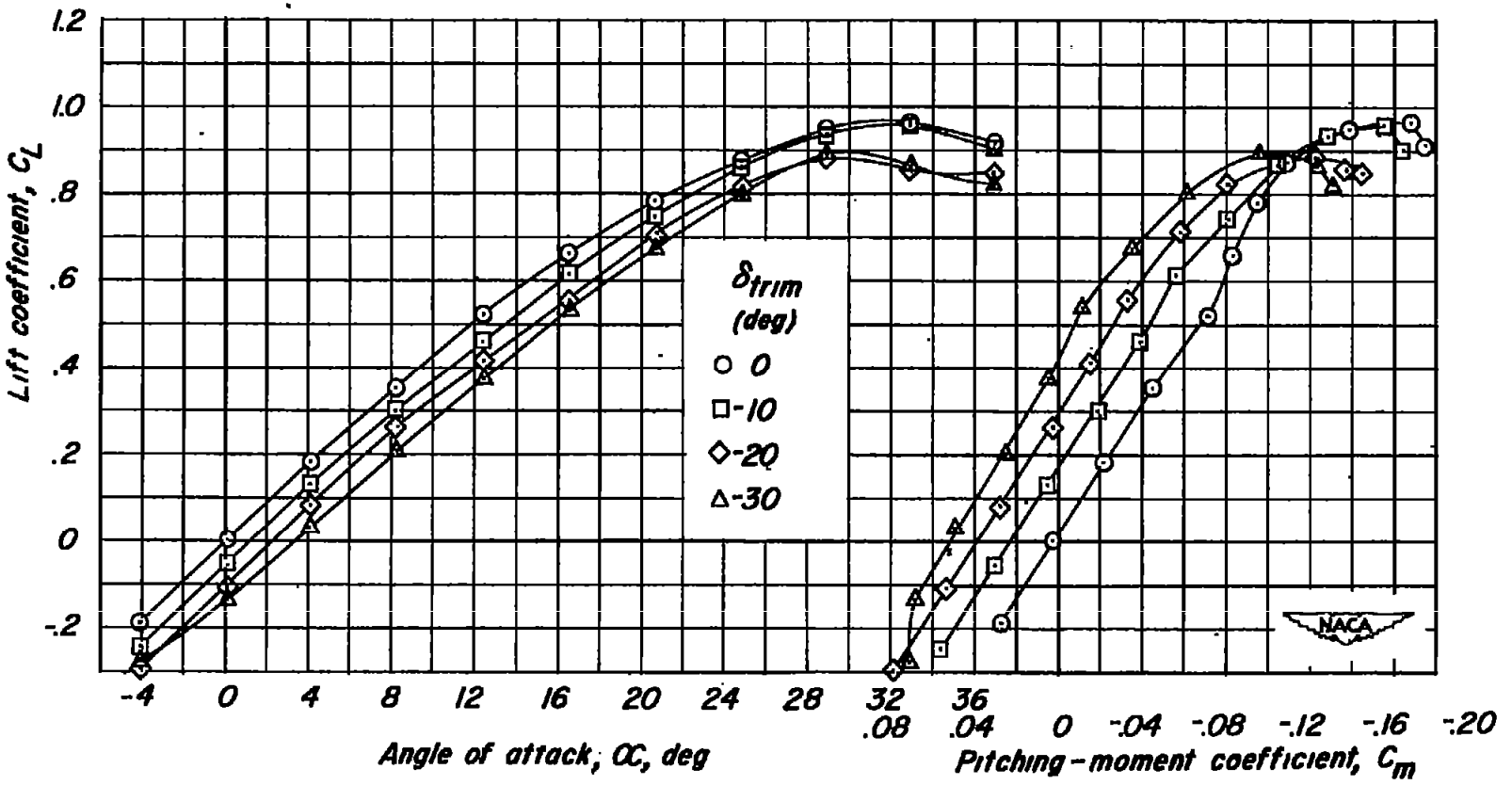

(d) $\frac{S_c}{S_w} = 0.10$; circular end plates.

Figure 4.- Concluded.

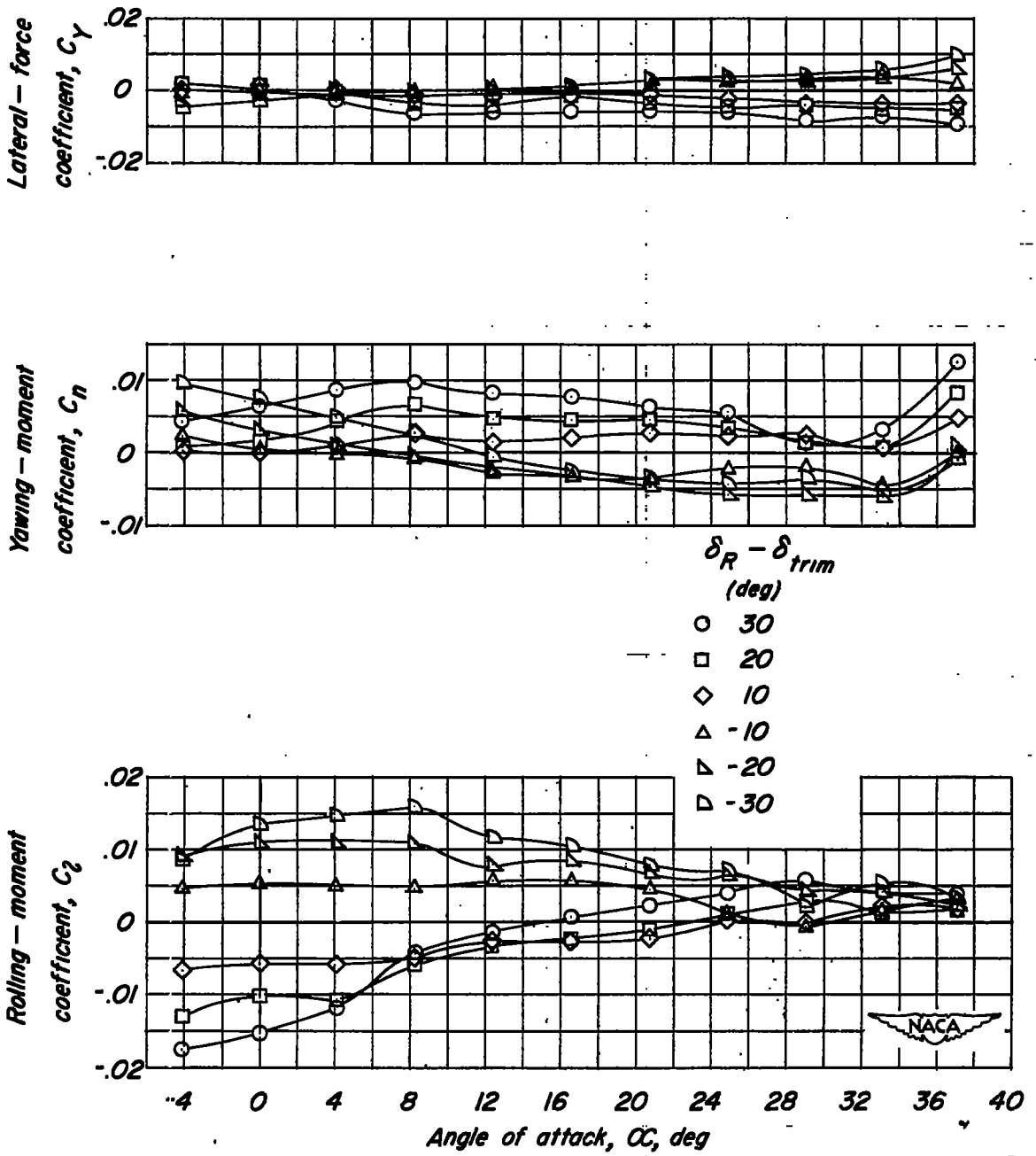

(a) $\delta_{trim} = 0°$.

Figure 5.- Lateral control characteristics of a 60° triangular-wing model having half-delta tip controls. $\frac{S_c}{S_w} = 0.05$.

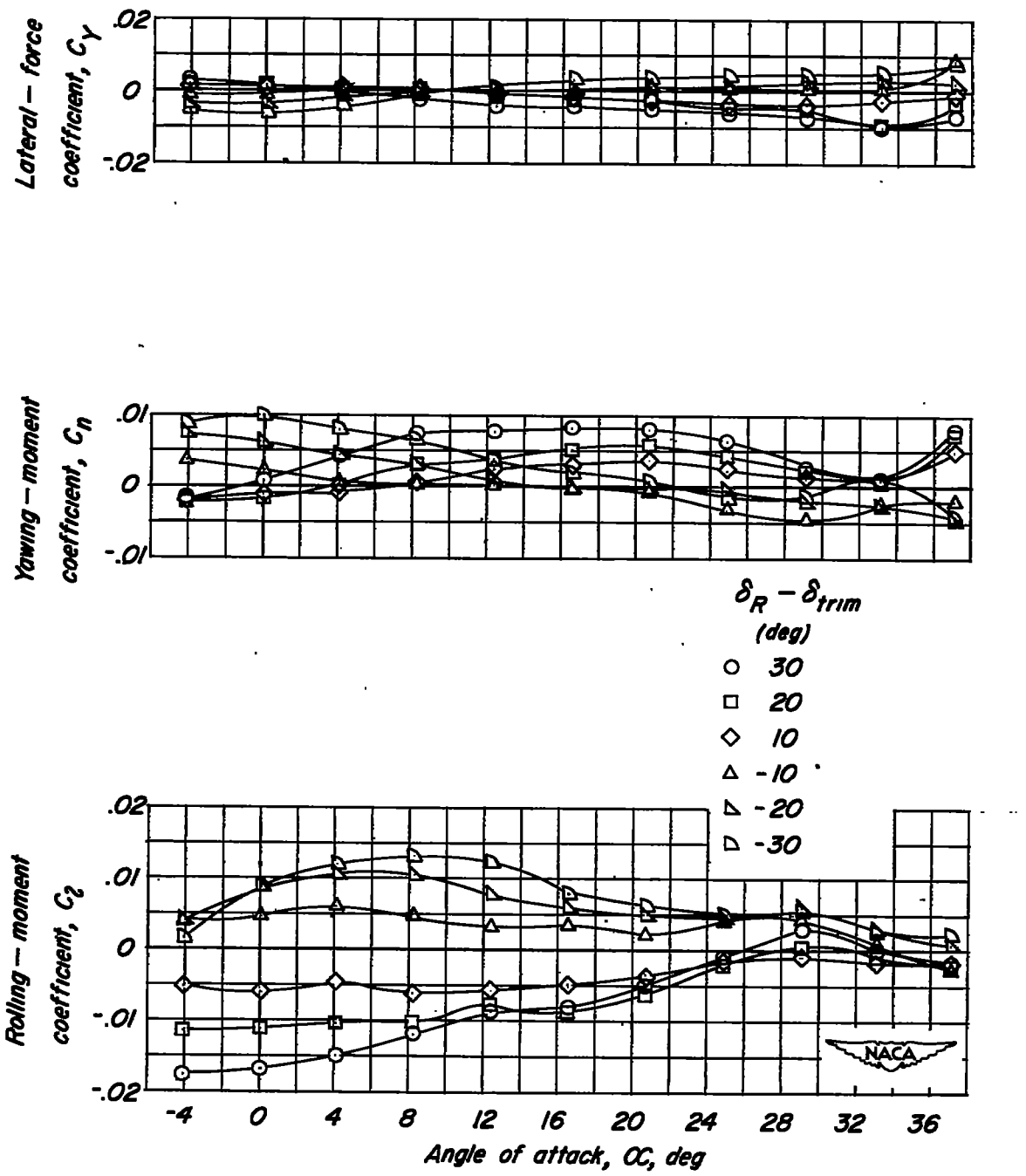

(b) $\delta_{trim} = -10^\circ$.

Figure 5.- Continued.

[redacted]

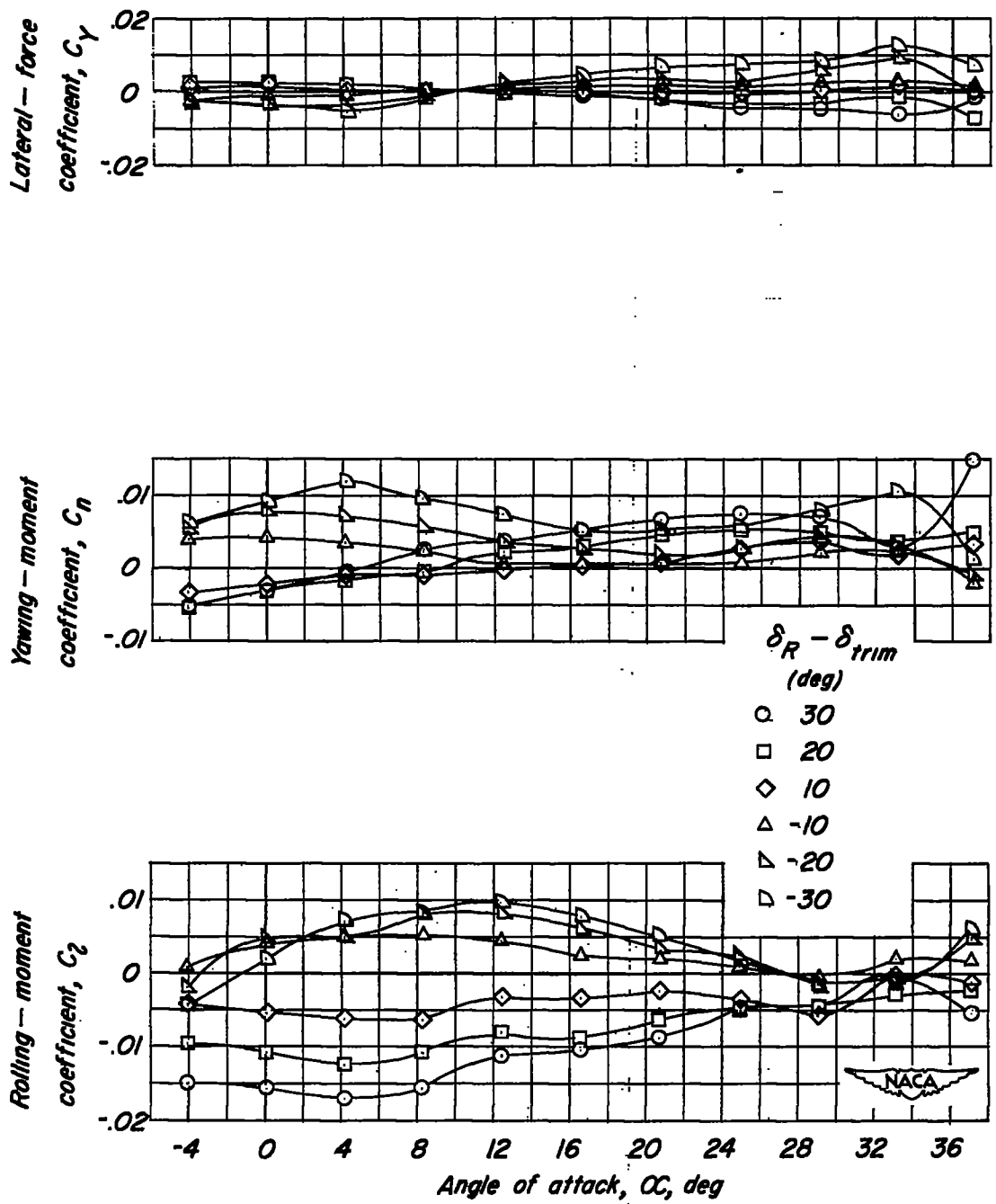

(c) $\delta_{trim} = -20°$.

Figure 5.- Continued.

[redacted]

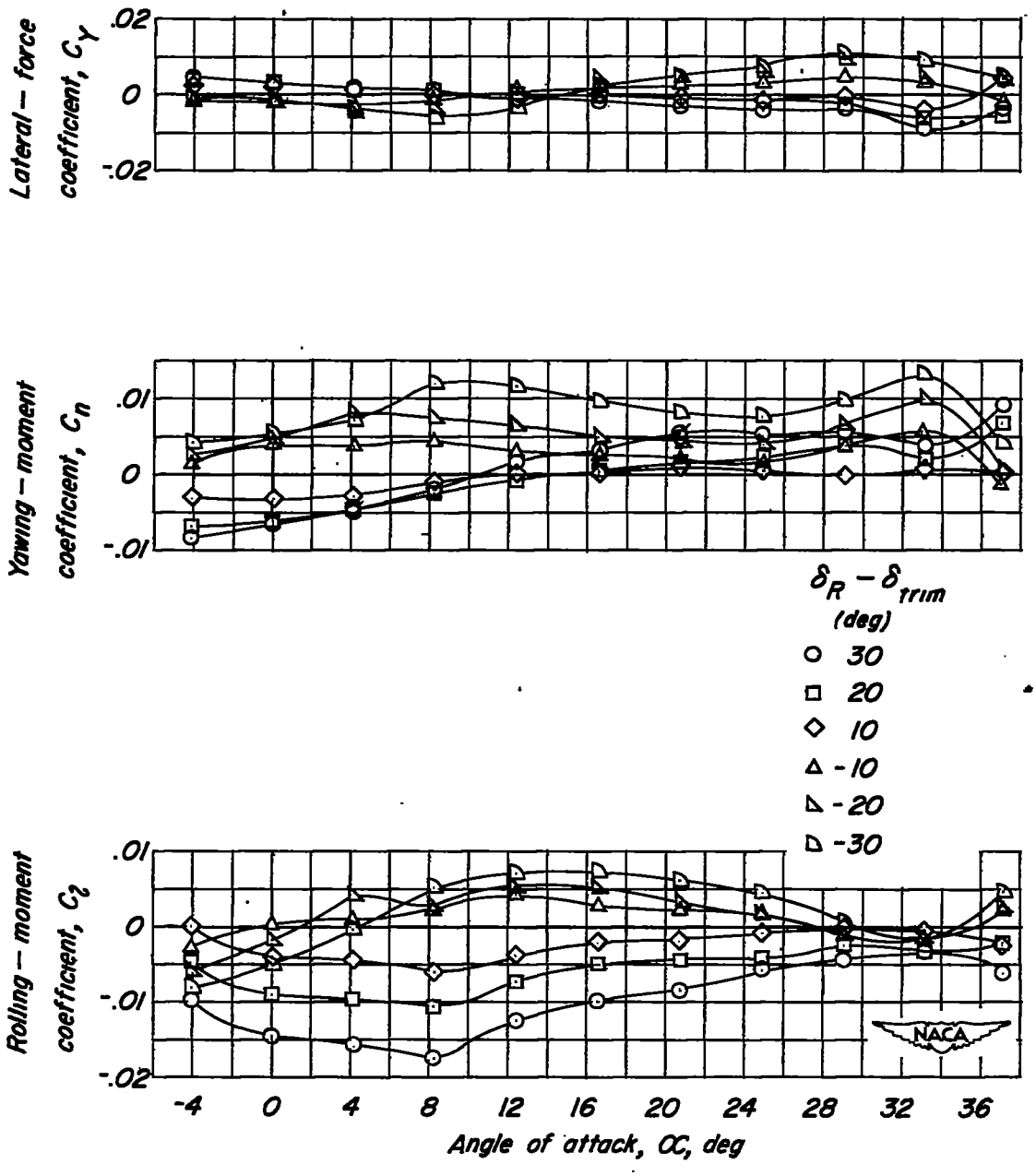

(d) $\delta_{trim} = -30°$.

Figure 5.- Concluded.

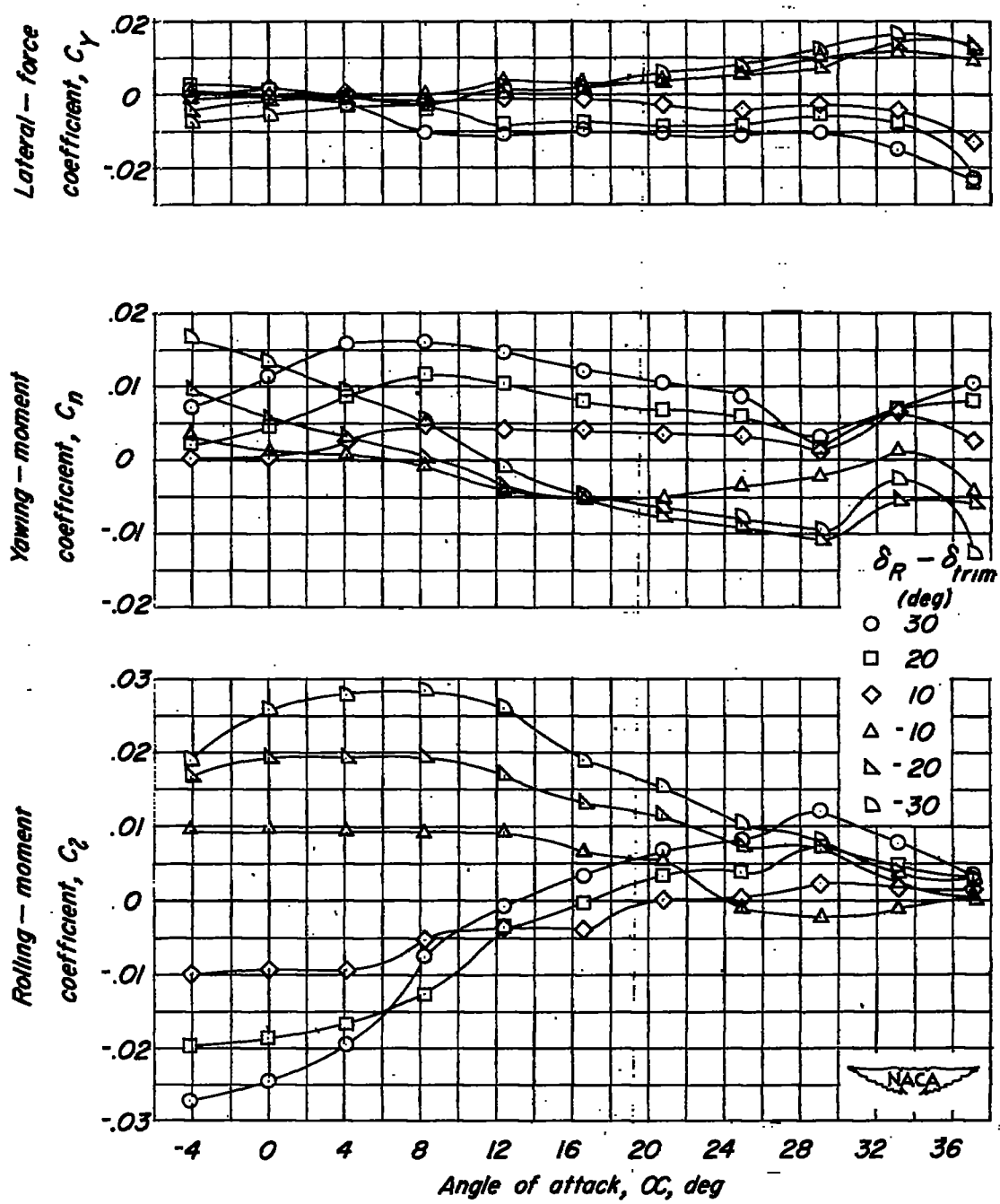

(a) $\delta_{trim} = 0^\circ$.

Figure 6.- Lateral control characteristics of a 60° triangular-wing model having half-delta tip controls. $\frac{S_c}{S_w} = 0.10$.

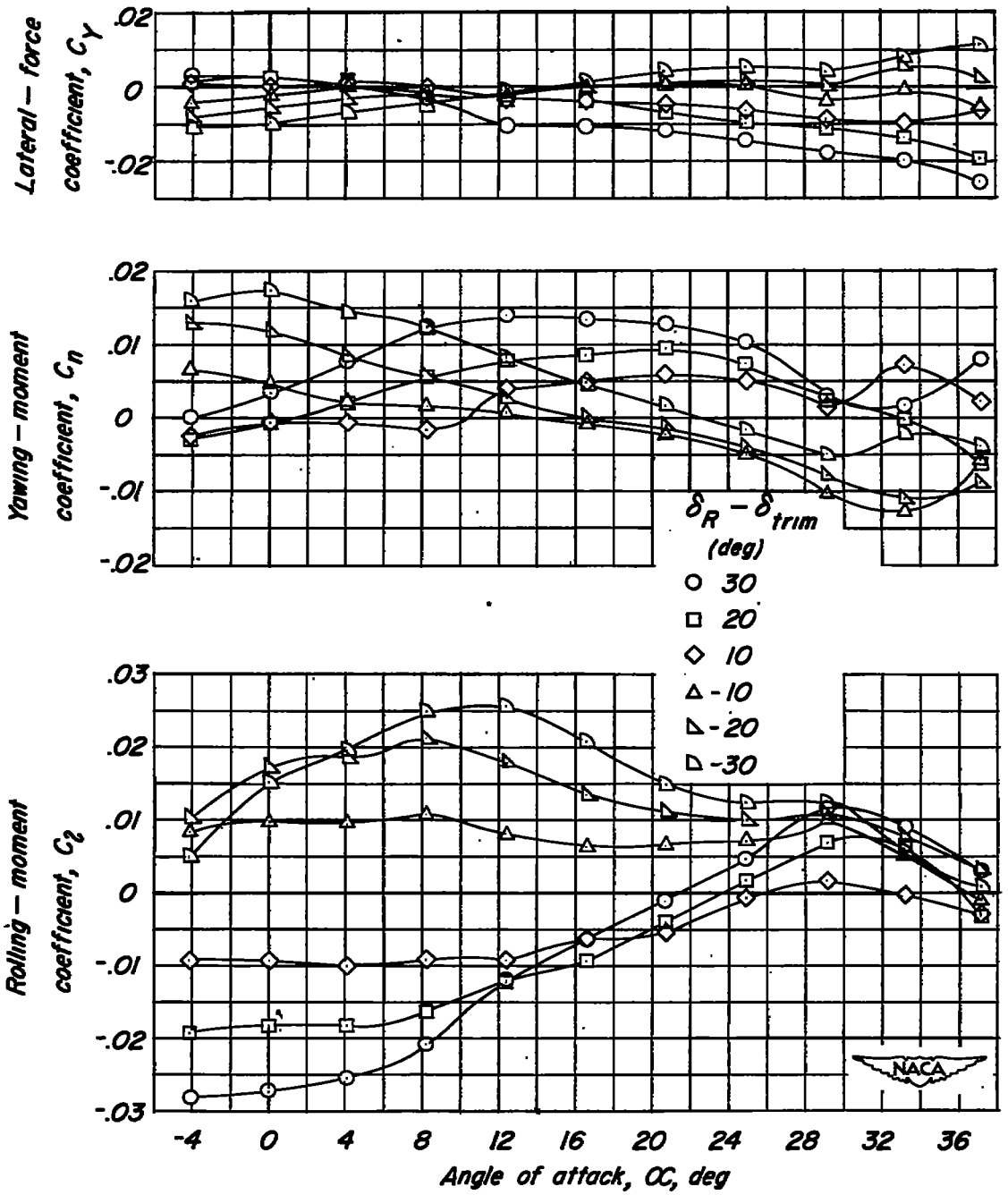

(b) $\delta_{trim} = -10°$.

Figure 6.- Continued.

[redacted]

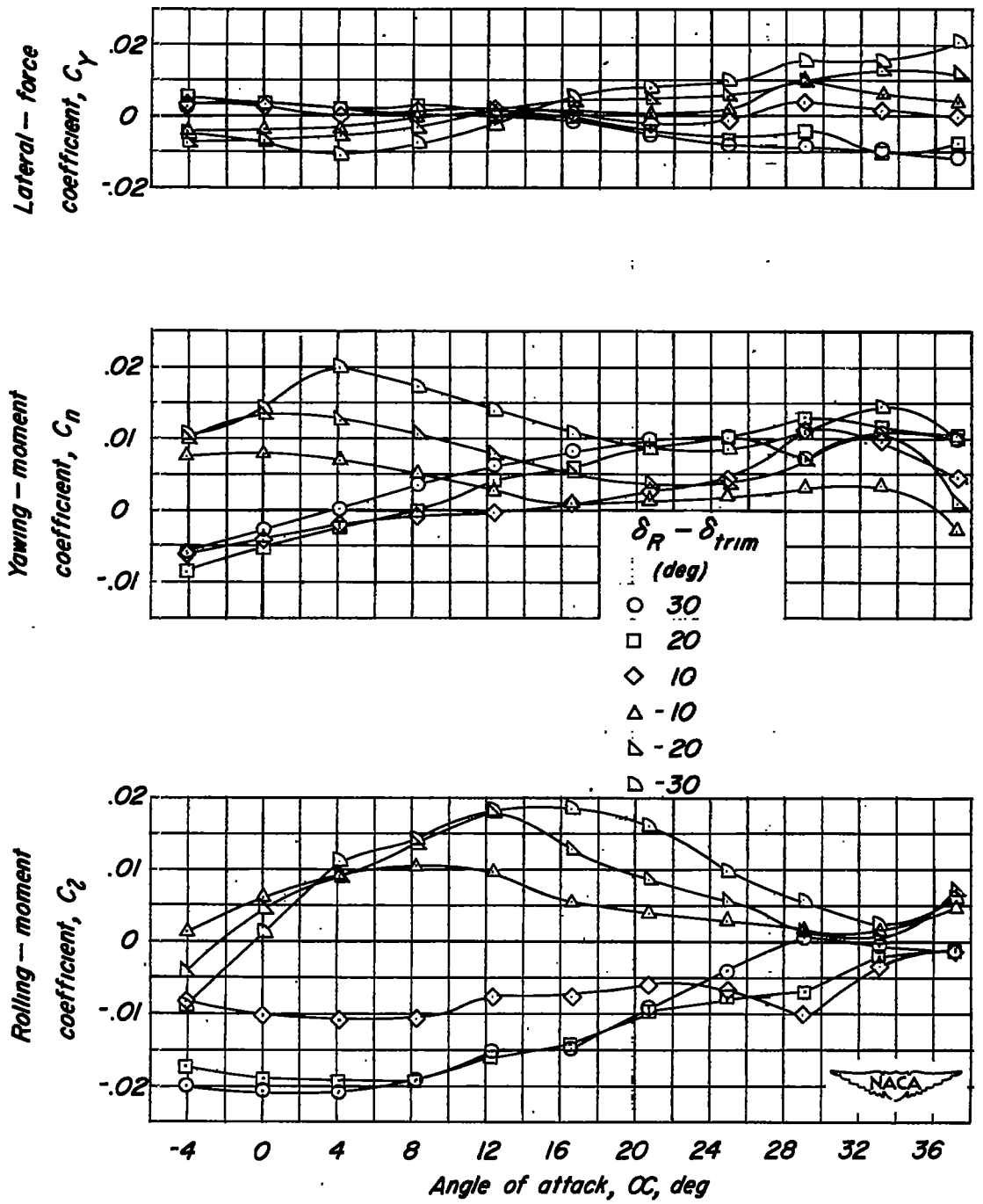

(c) $\delta_{trim} = -20°$.

Figure 6.- Continued.

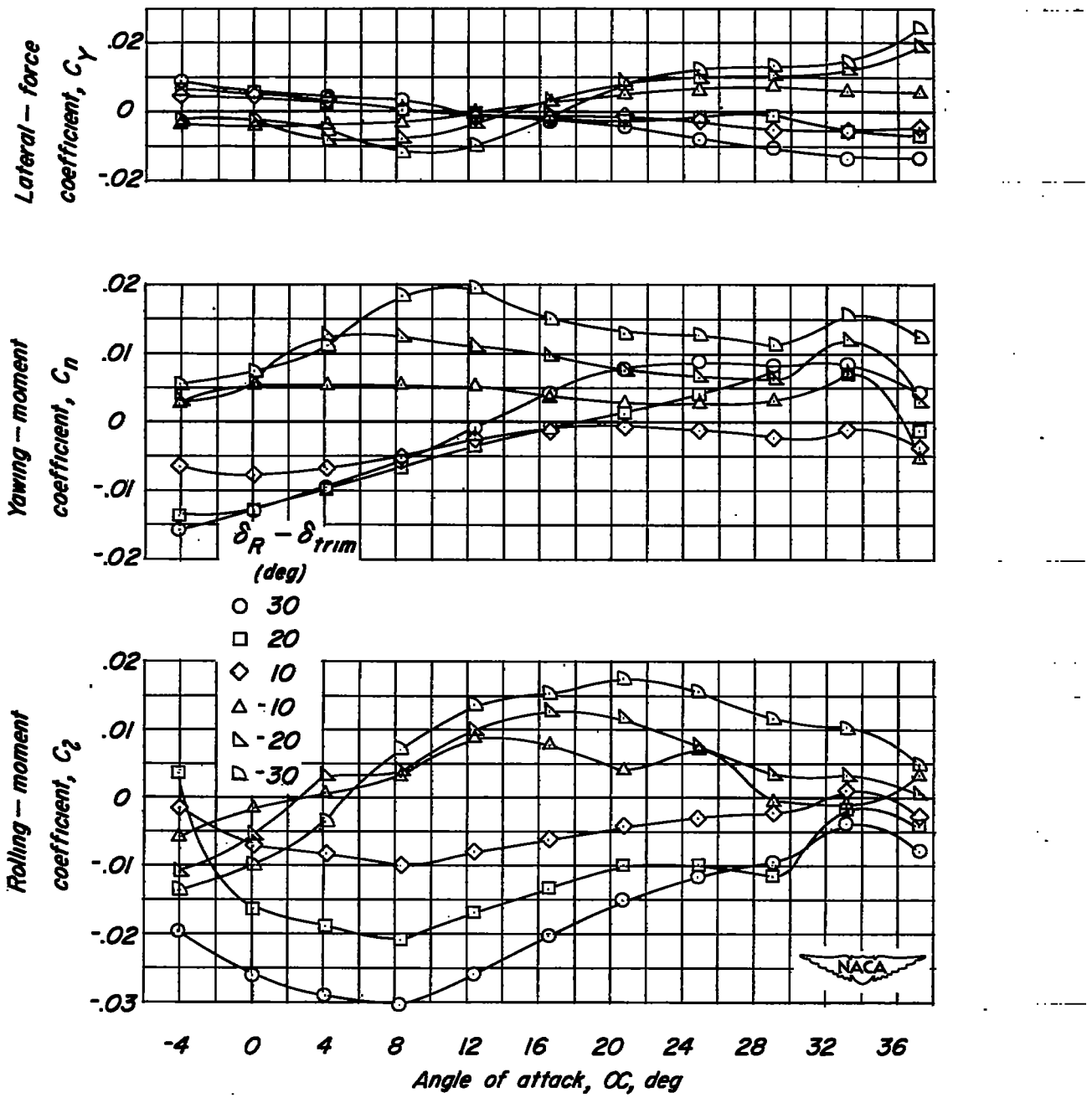

(d) $\delta_{trim} = -30^\circ$.

Figure 6.- Concluded.

[redacted]

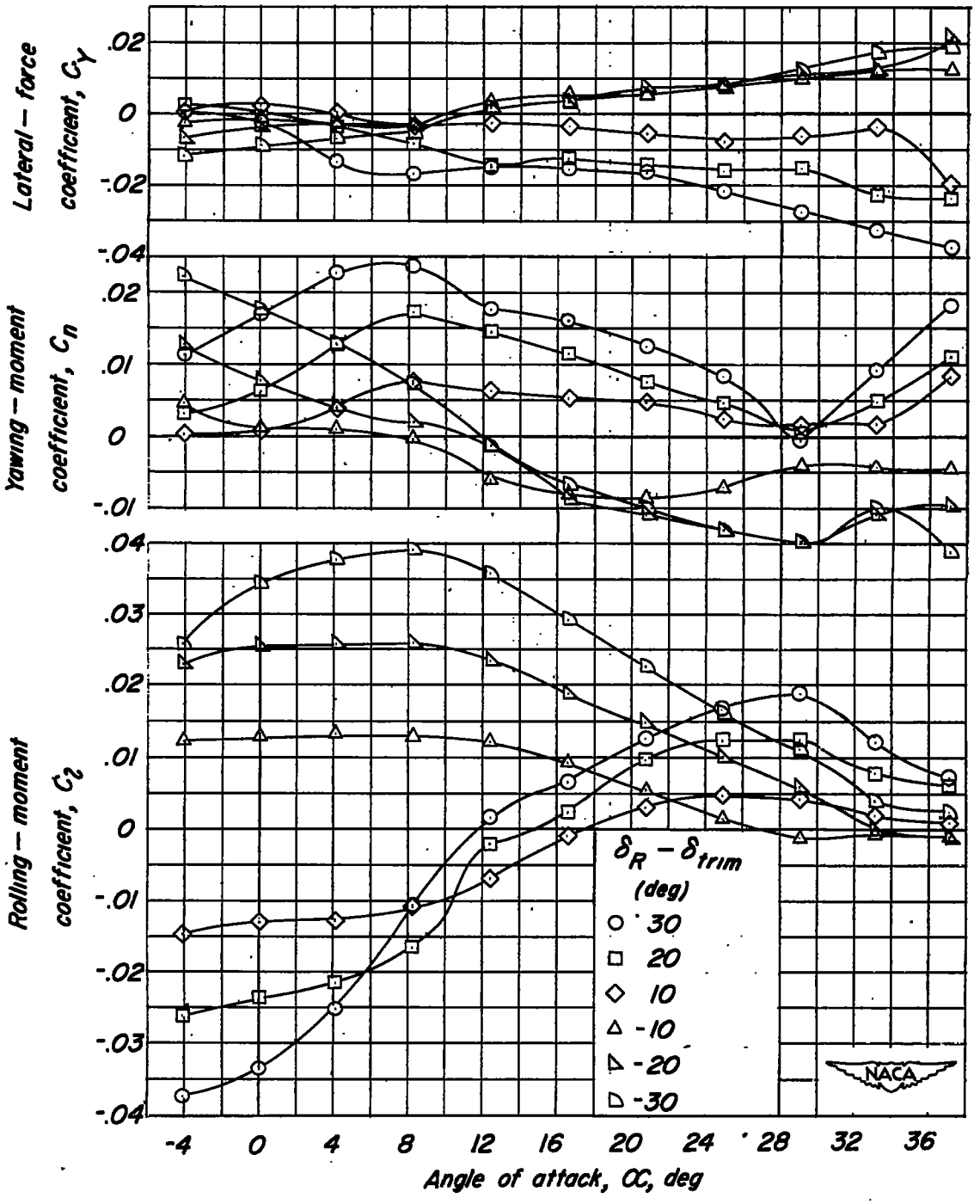

(a) $\delta_{trim} = 0°$.

Figure 7.- Lateral control characteristics of a 60° triangular-wing model having half-delta tip controls. $\frac{S_c}{S_w} = 0.15$.

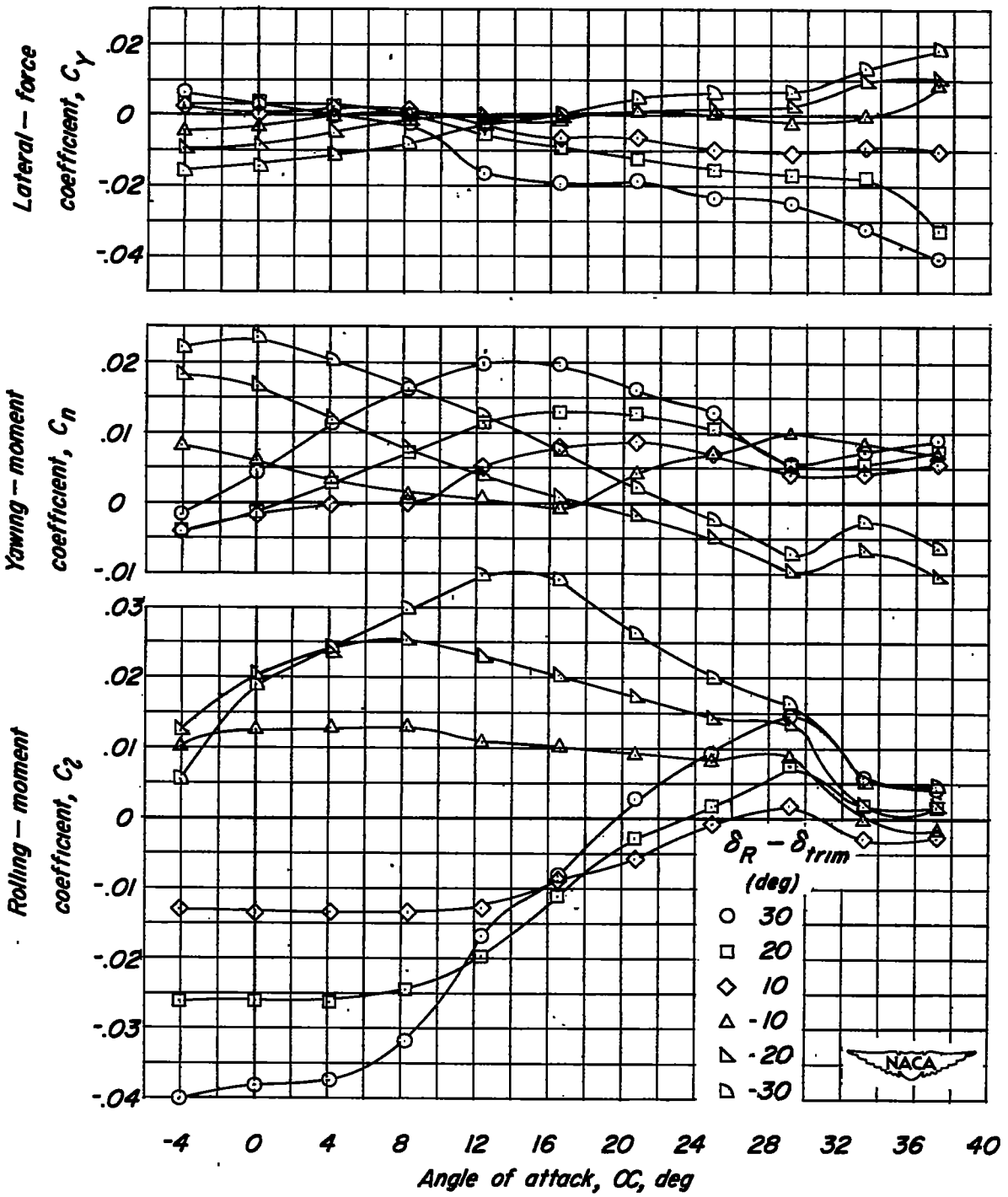

(b) $\delta_{trim} = -10°$.

Figure 7.- Continued.

[redacted]

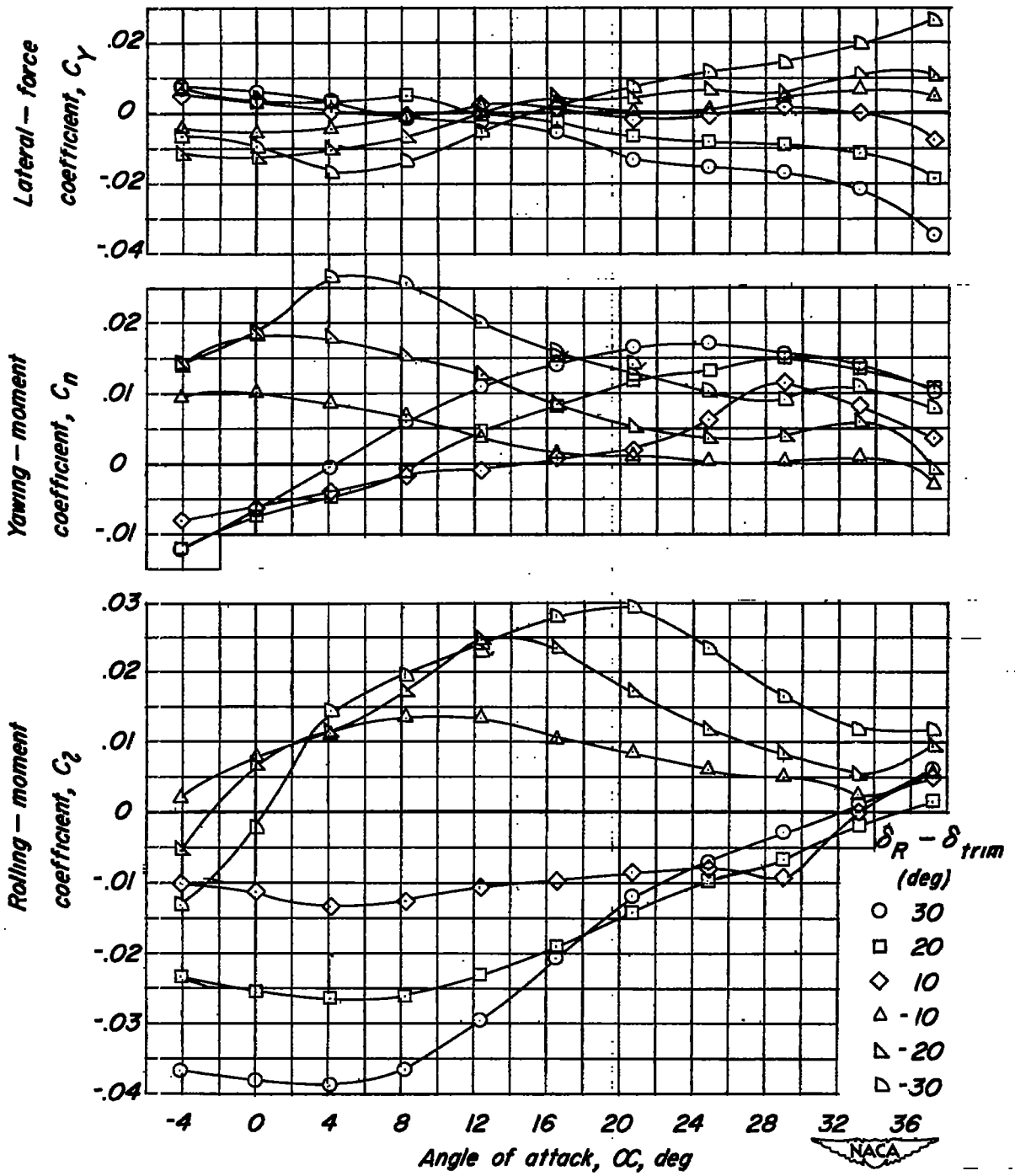

(c) $\delta_{trim} = -20°$.

Figure 7.- Continued.

[redacted]

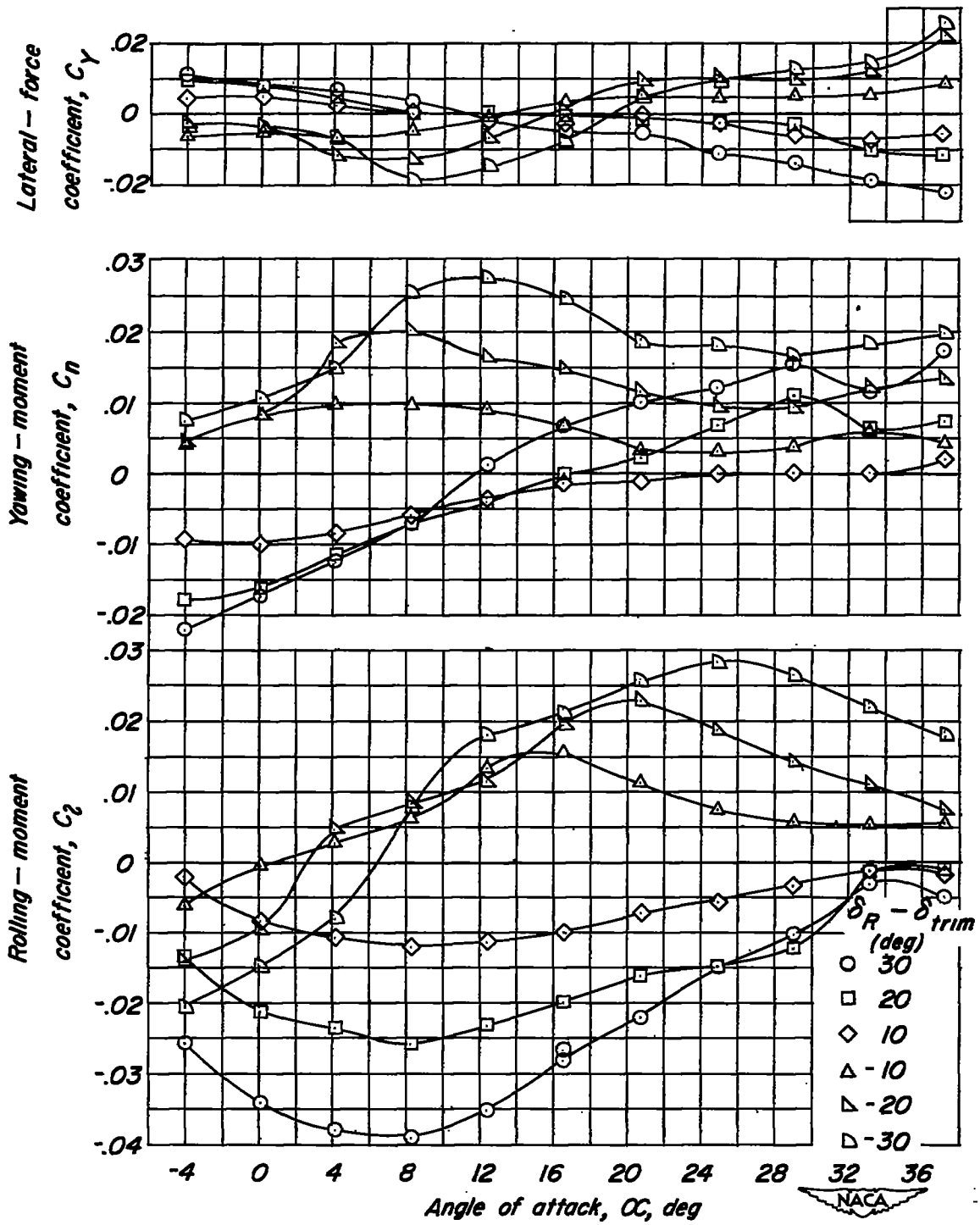

(d) $\delta_{trim} = -30°$.

Figure 7.- Concluded.

[redacted]

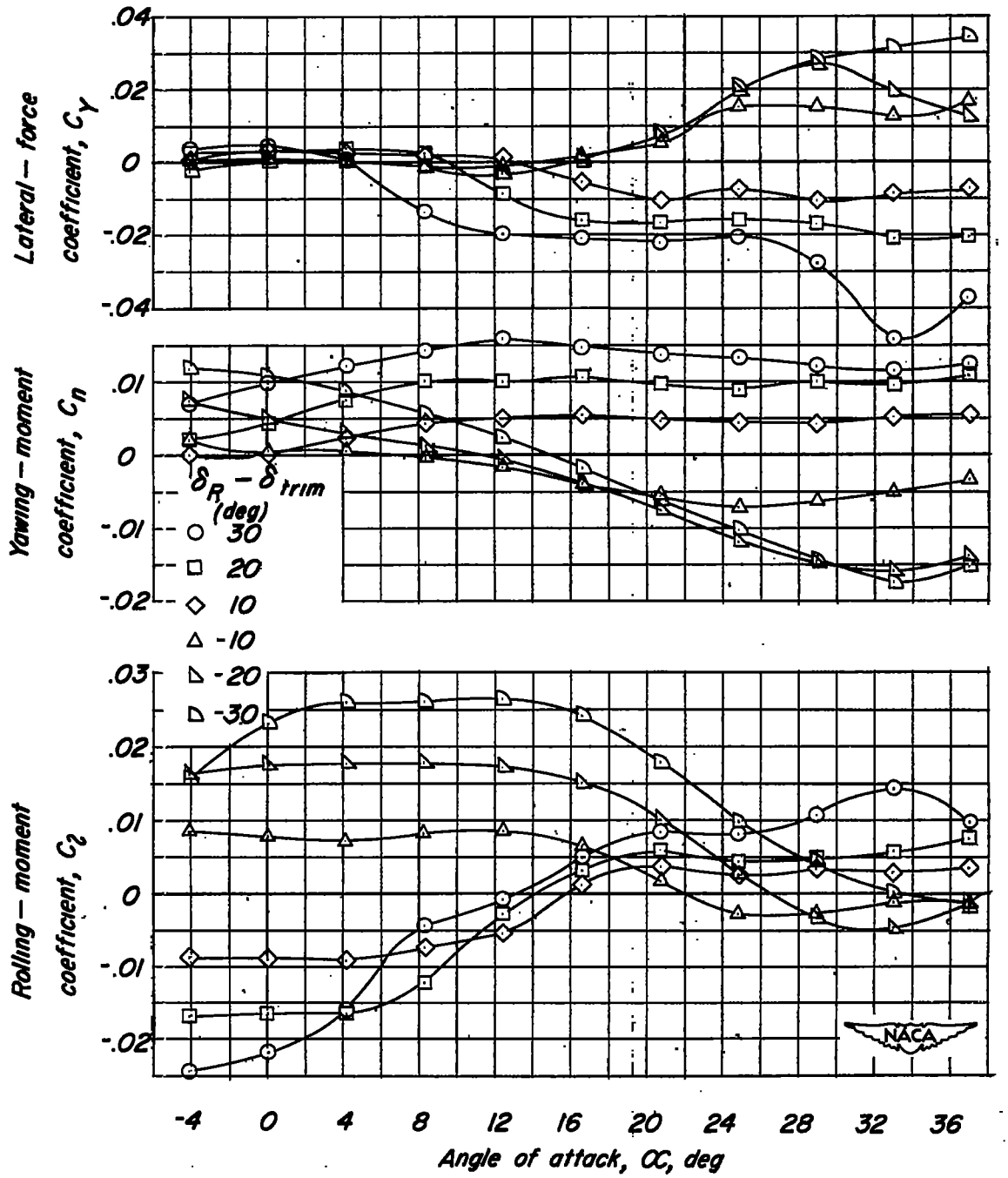

(a) $\delta_{trim} = 0°$.

Figure 8.- Lateral control characteristics of a 60° triangular-wing model having half-delta tip controls and circular end plates. $\frac{S_c}{S_w} = 0.10$.

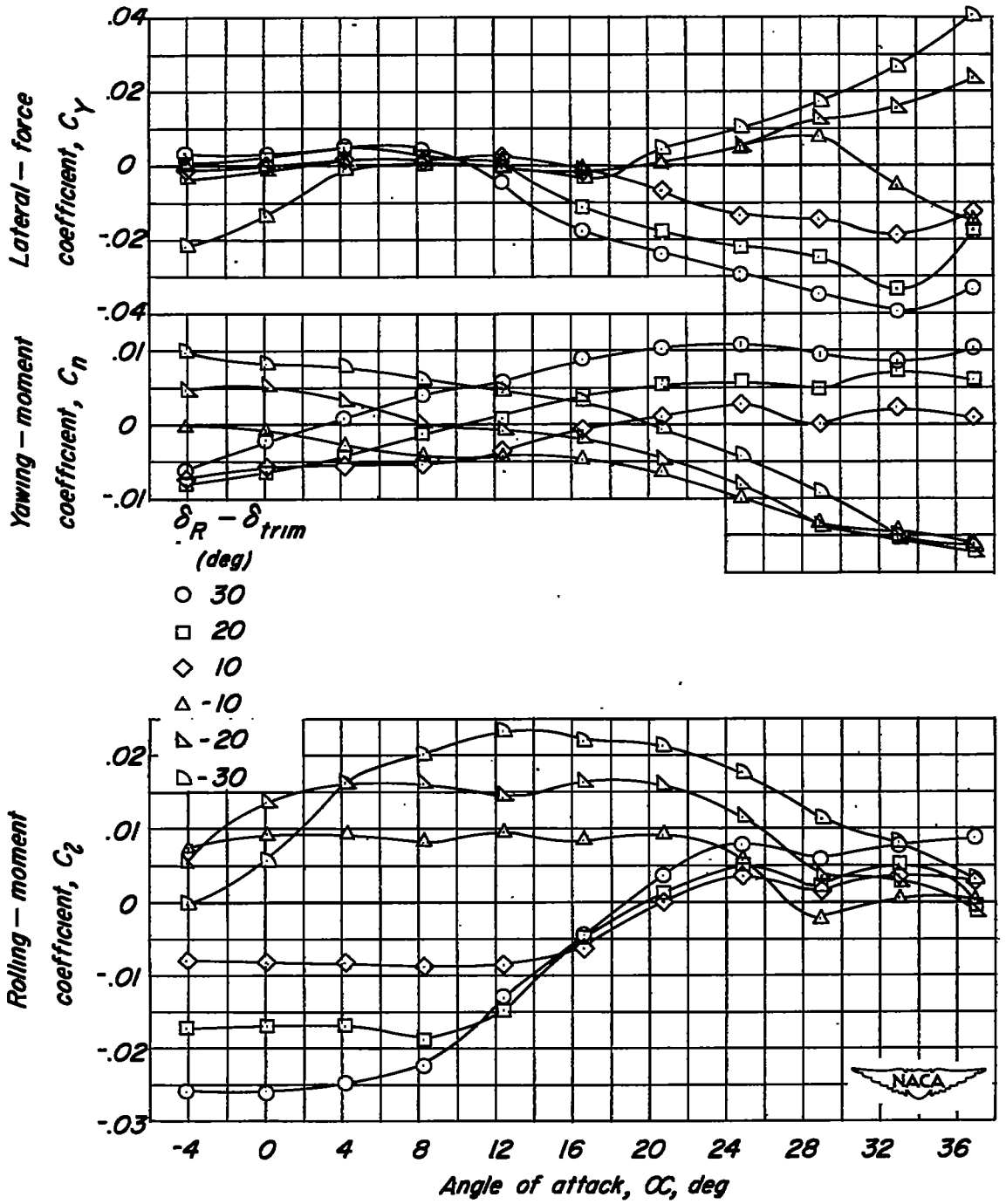

(b) $\delta_{trim} = -10^\circ$.

Figure 8.- Continued.

[redacted]

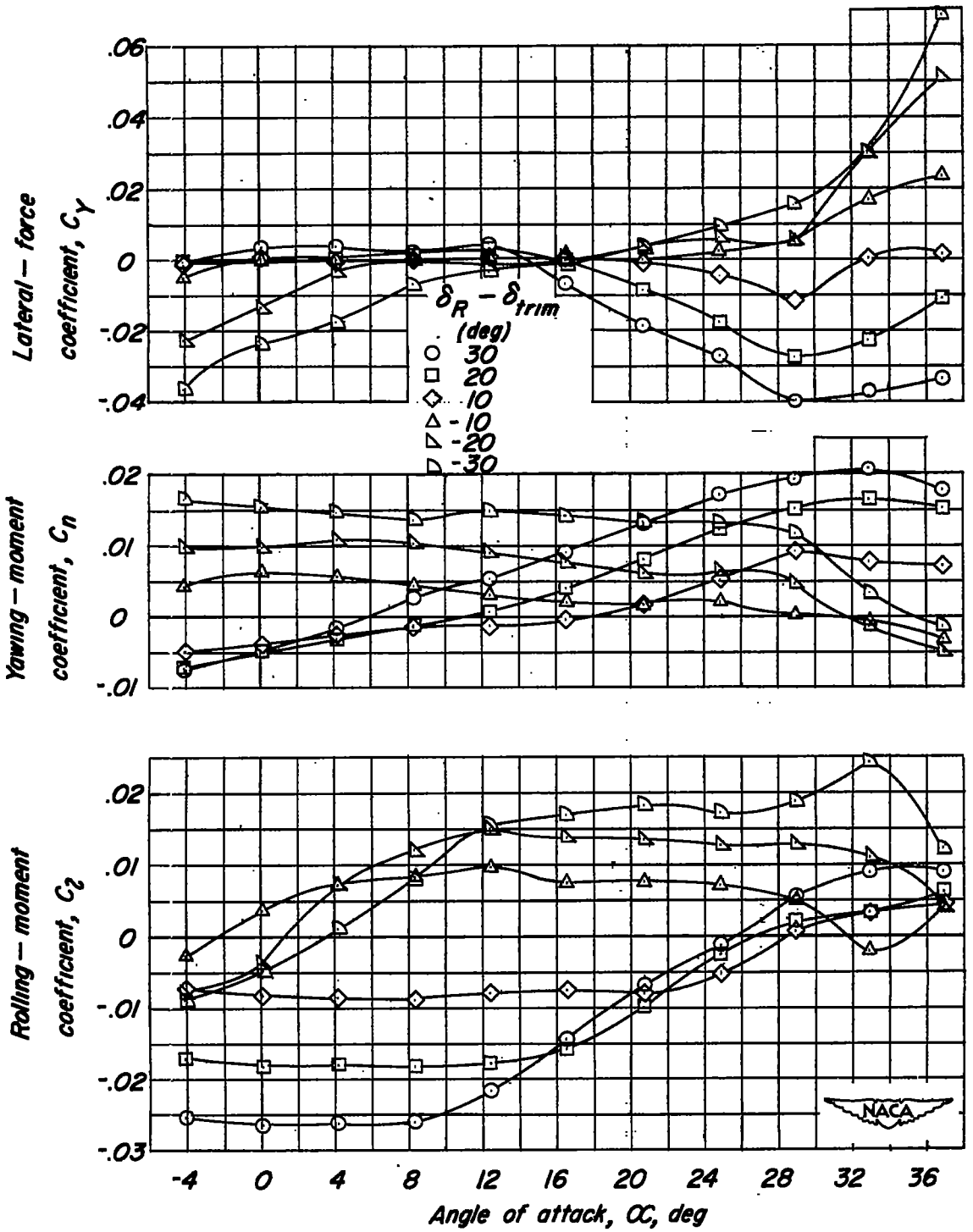

(c) $\delta_{trim} = -20^\circ$.

Figure 8.- Continued.

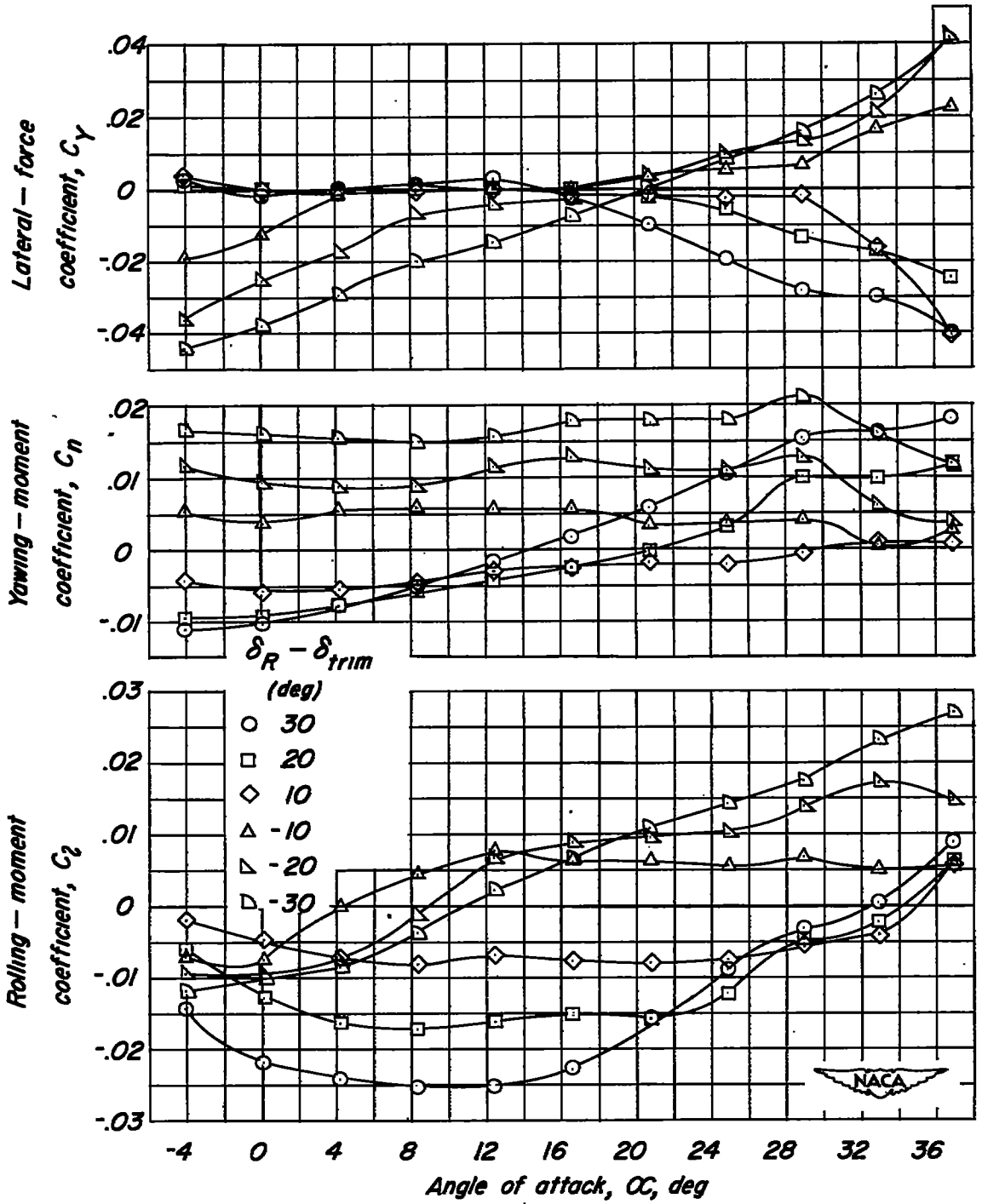

(d) $\delta_{trim} = -30°$.

Figure 8.- Concluded.

[redacted]

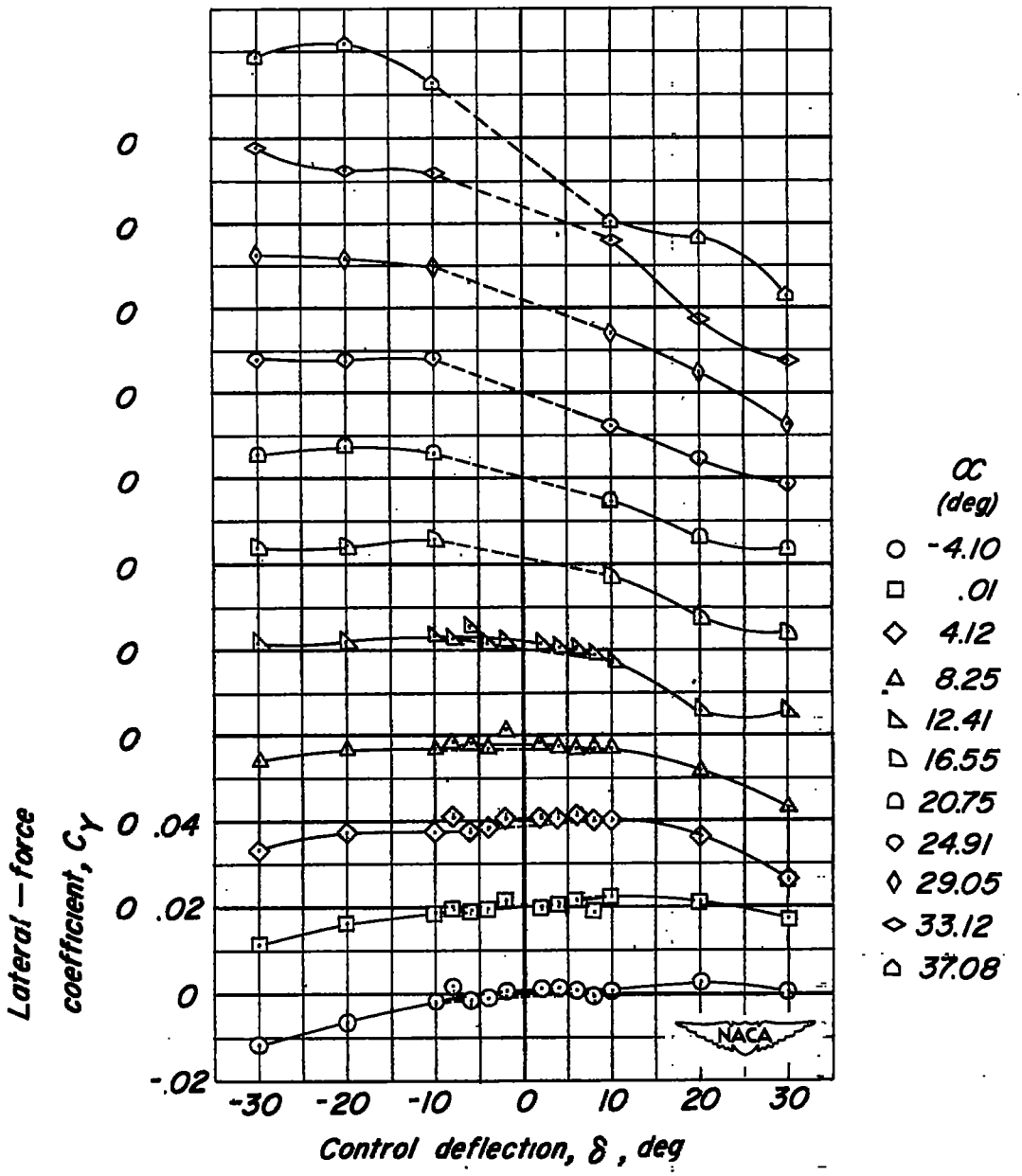

Figure 9.- Variation of C_Y, C_n, and C_l with control deflection and angle of attack for a 60° triangular-wing model having half-delta tip controls. $\frac{S_c}{S_w}$ = 0.15. Control parameters measured between control deflections of 10° and -10° as indicated by dashed lines. δ_{trim} = 0°.

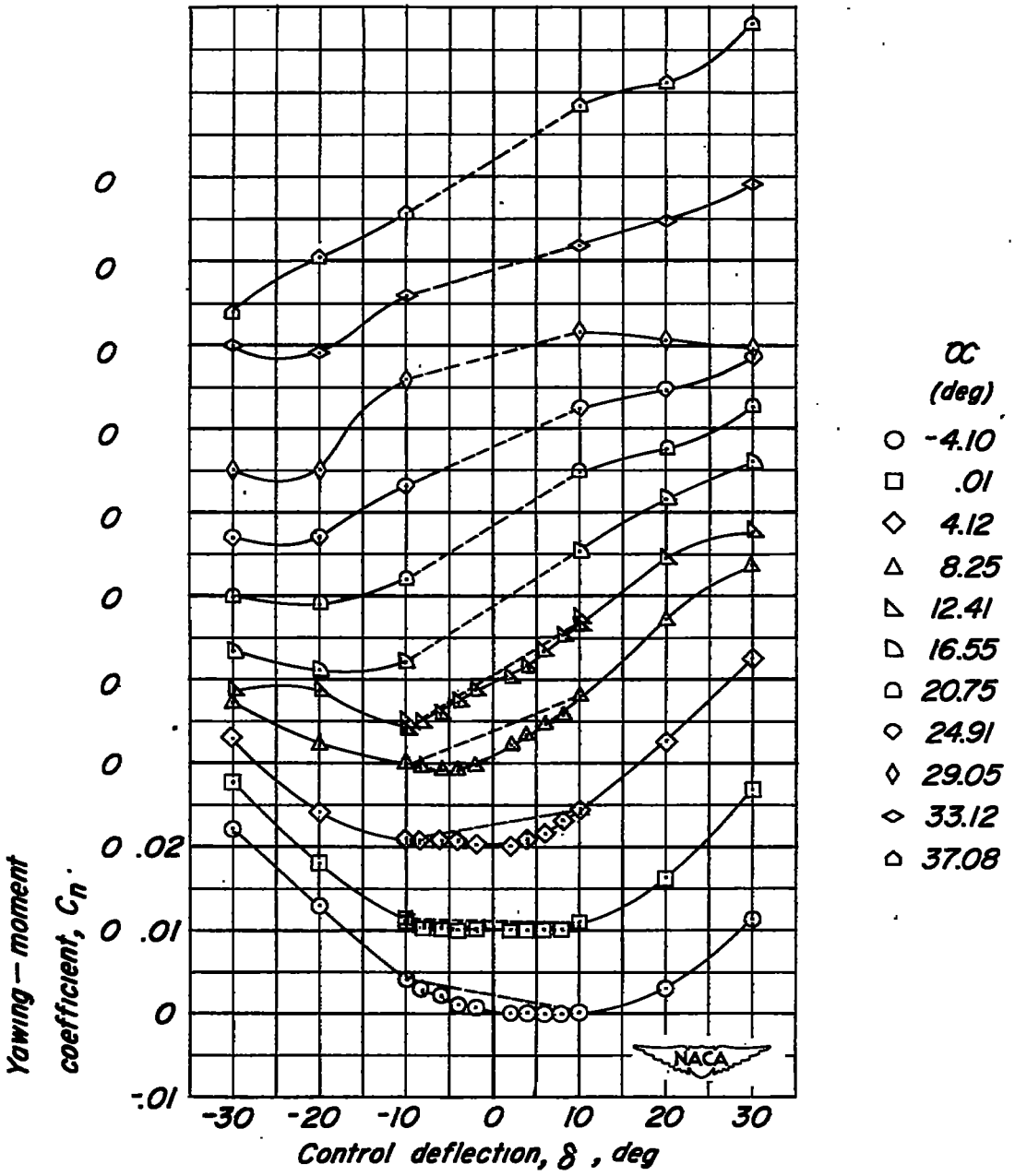

Figure 9.- Continued.

[redacted]

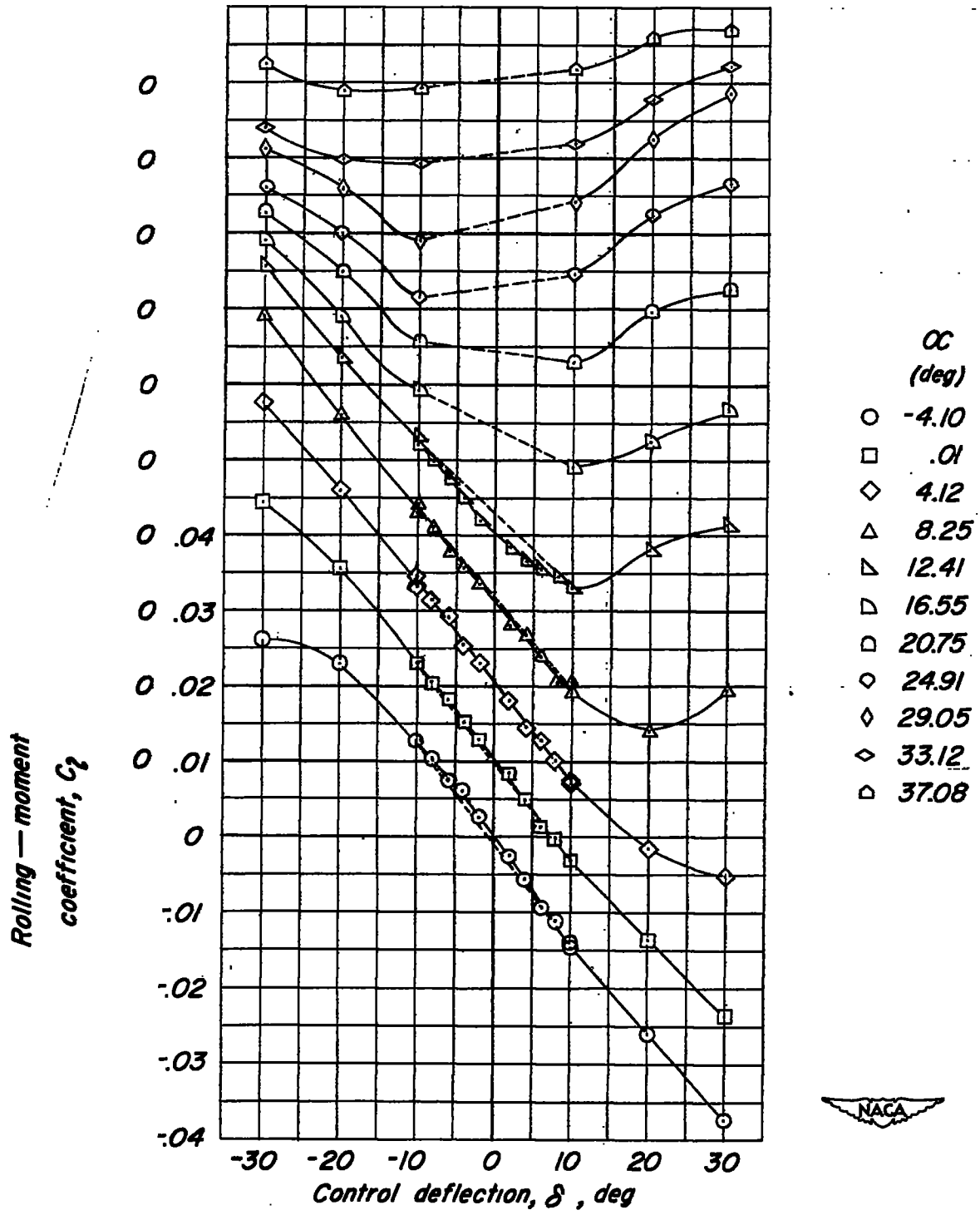

Figure 9.- Concluded.

[redacted]

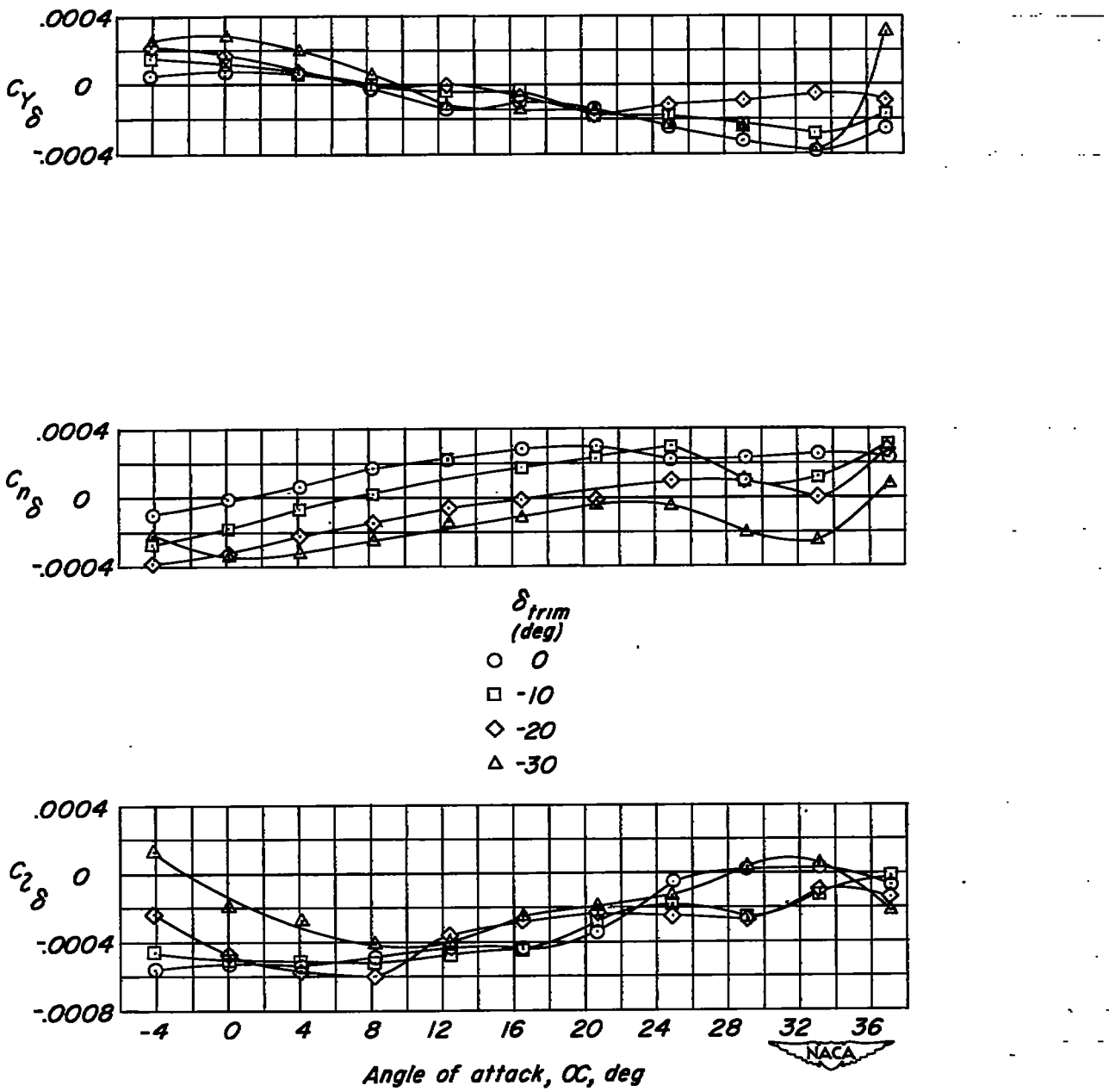

(a) $\frac{S_c}{S_w} = 0.05$.

Figure 10.- Variation of C_{Y_δ}, C_{n_δ}, and C_{l_δ} with angle of attack for several symmetrical control deflections for a 60° triangular-wing model having half-delta tip controls.

[redacted]

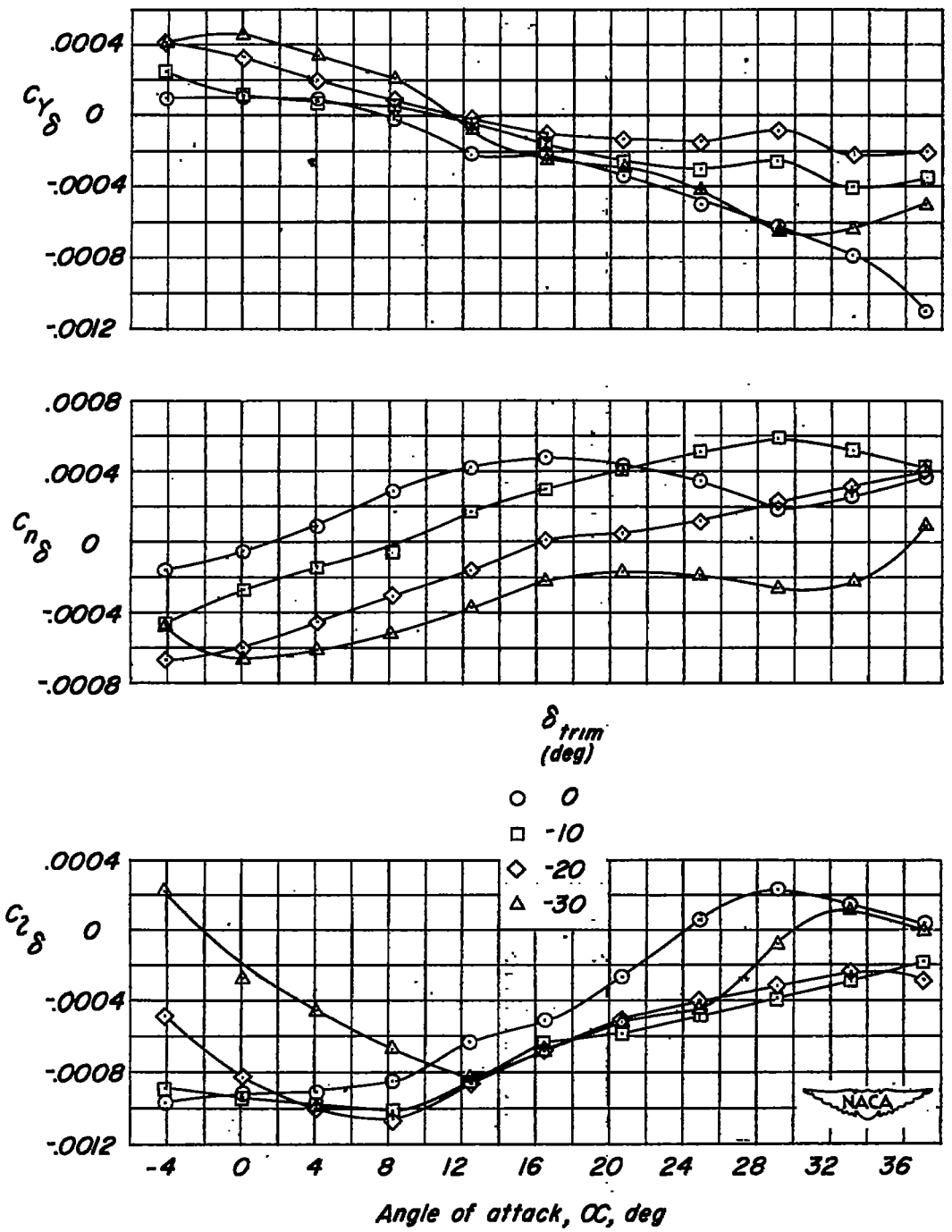

(b) $\frac{S_c}{S_w} = 0.10$.

Figure 10.- Continued.

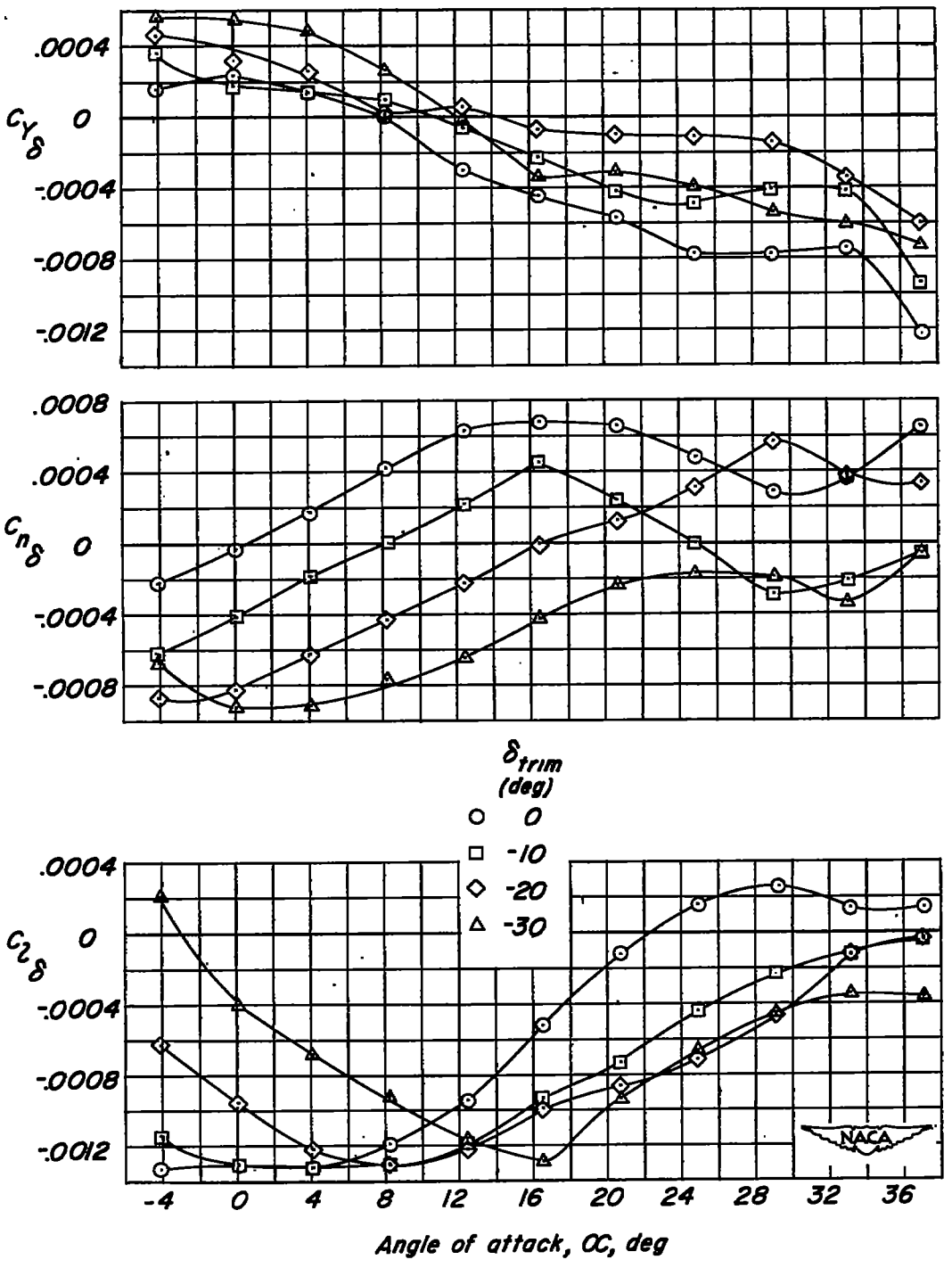

(c) $\frac{S_c}{S_w} = 0.15$.

Figure 10.- Continued.

[redacted]

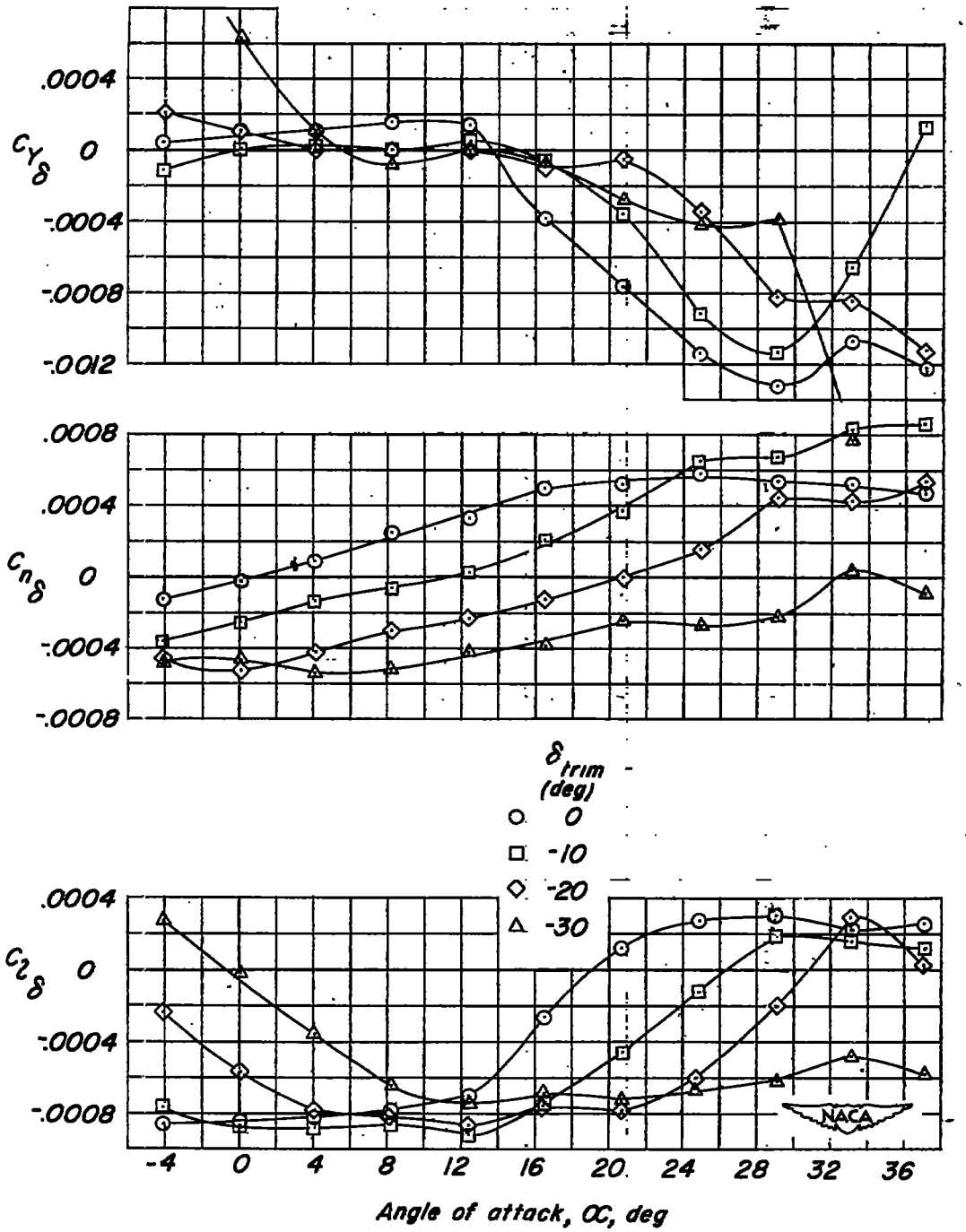

(d) $\frac{S_c}{S_w}$ = 0.10; circular end plates.

Figure 10.- Concluded.

[redacted]

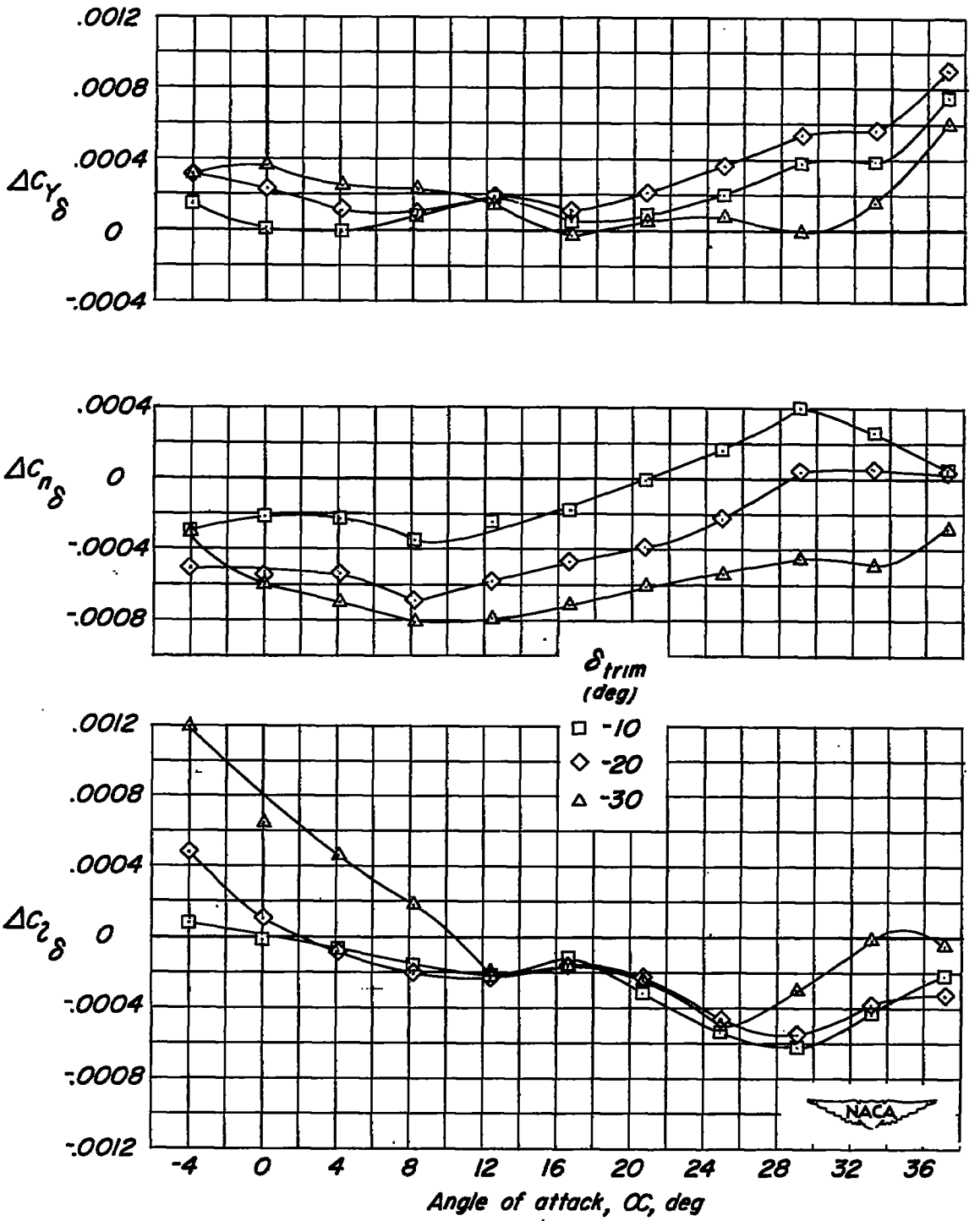

Figure 11.- Variation of ΔC_{Y_δ}, ΔC_{n_δ}, and ΔC_{l_δ} due to symmetrical control deflection with α for a 60° triangular-wing model having 10-percent half-delta tip controls.

[redacted]

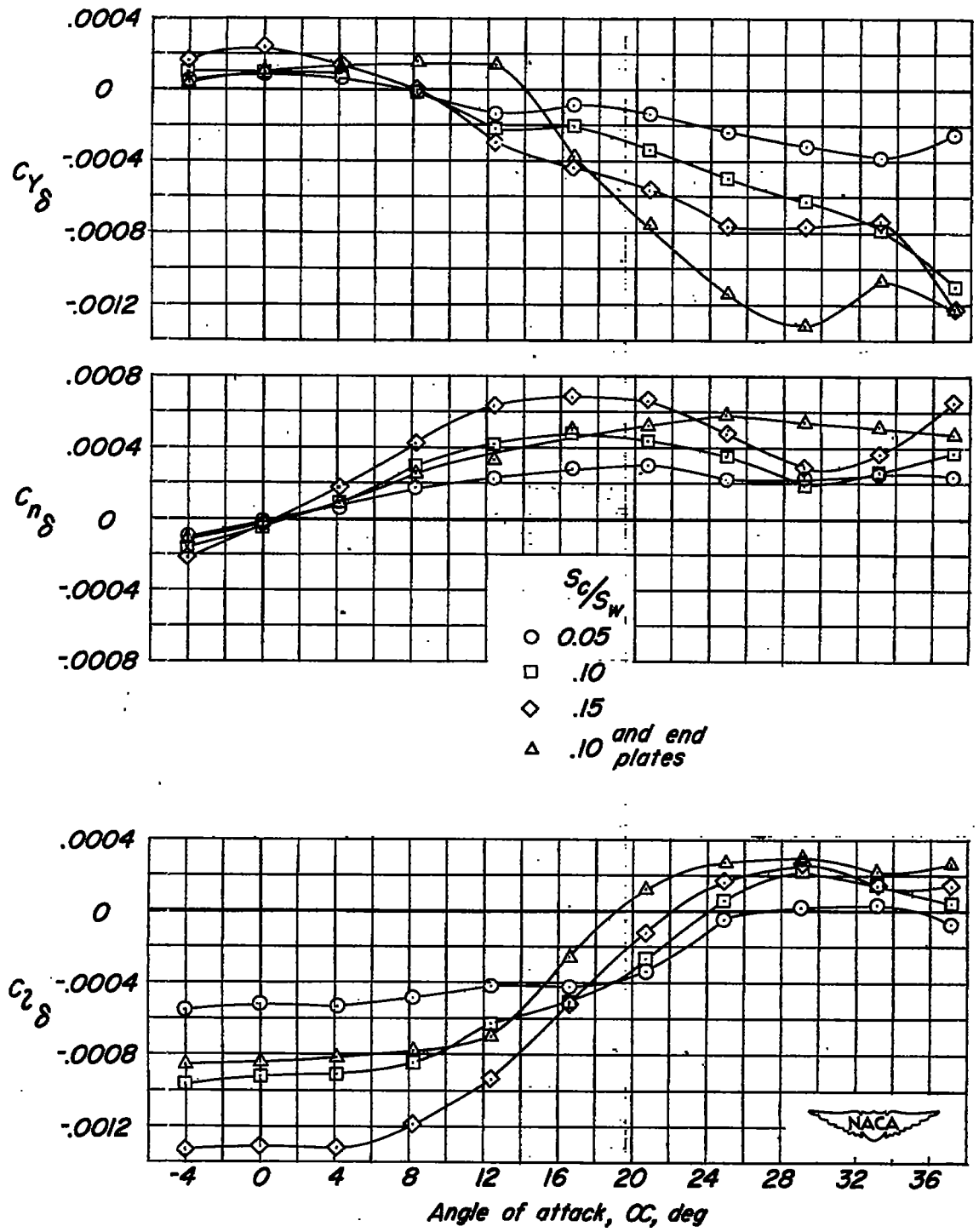

(a) $\delta_{trim} = 0°$.

Figure 12.- Lateral control characteristics of a 60° triangular-wing model having half-delta tip controls.

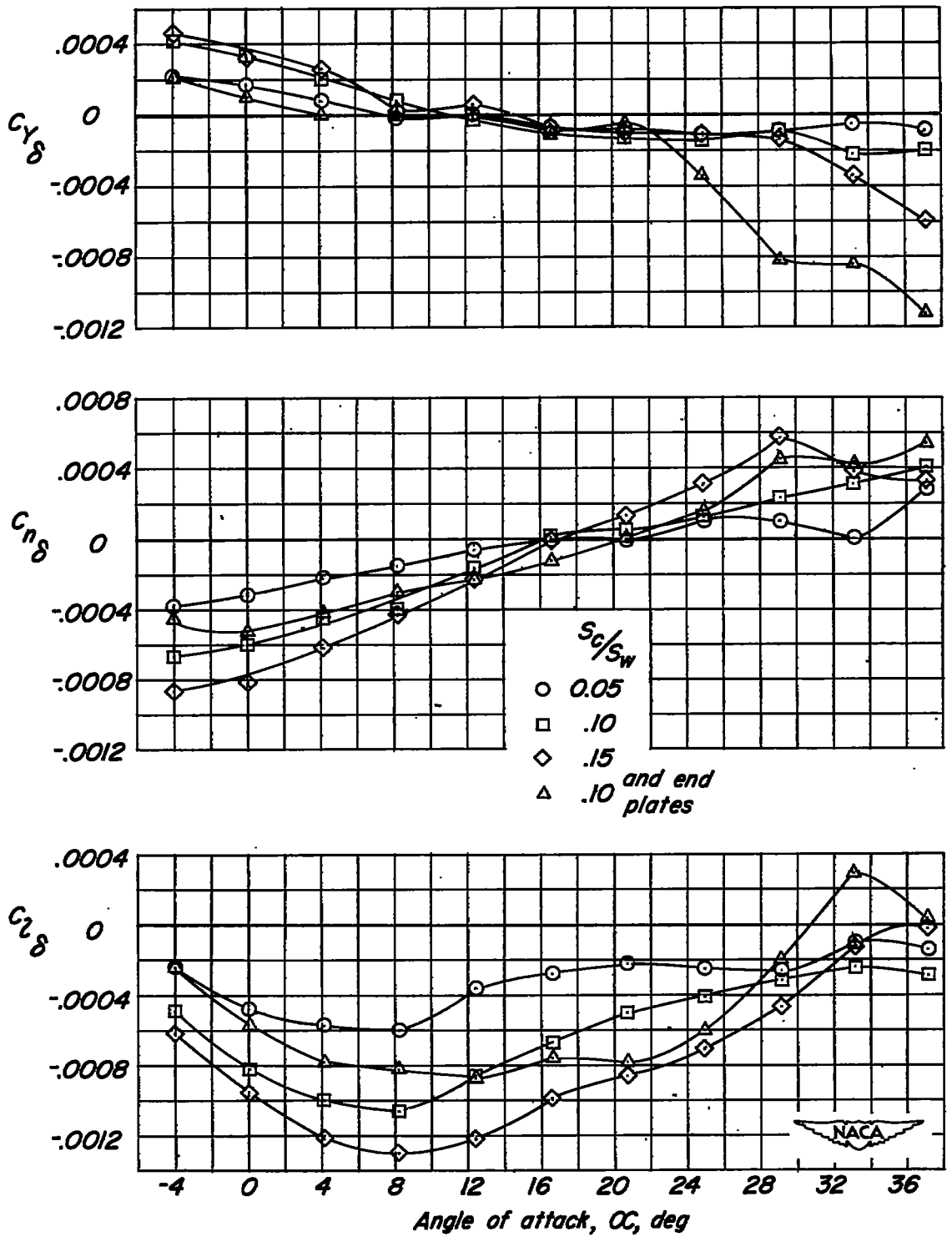

(b) $\delta_{trim} = -20^\circ$.

Figure 12.- Concluded.

[redacted]

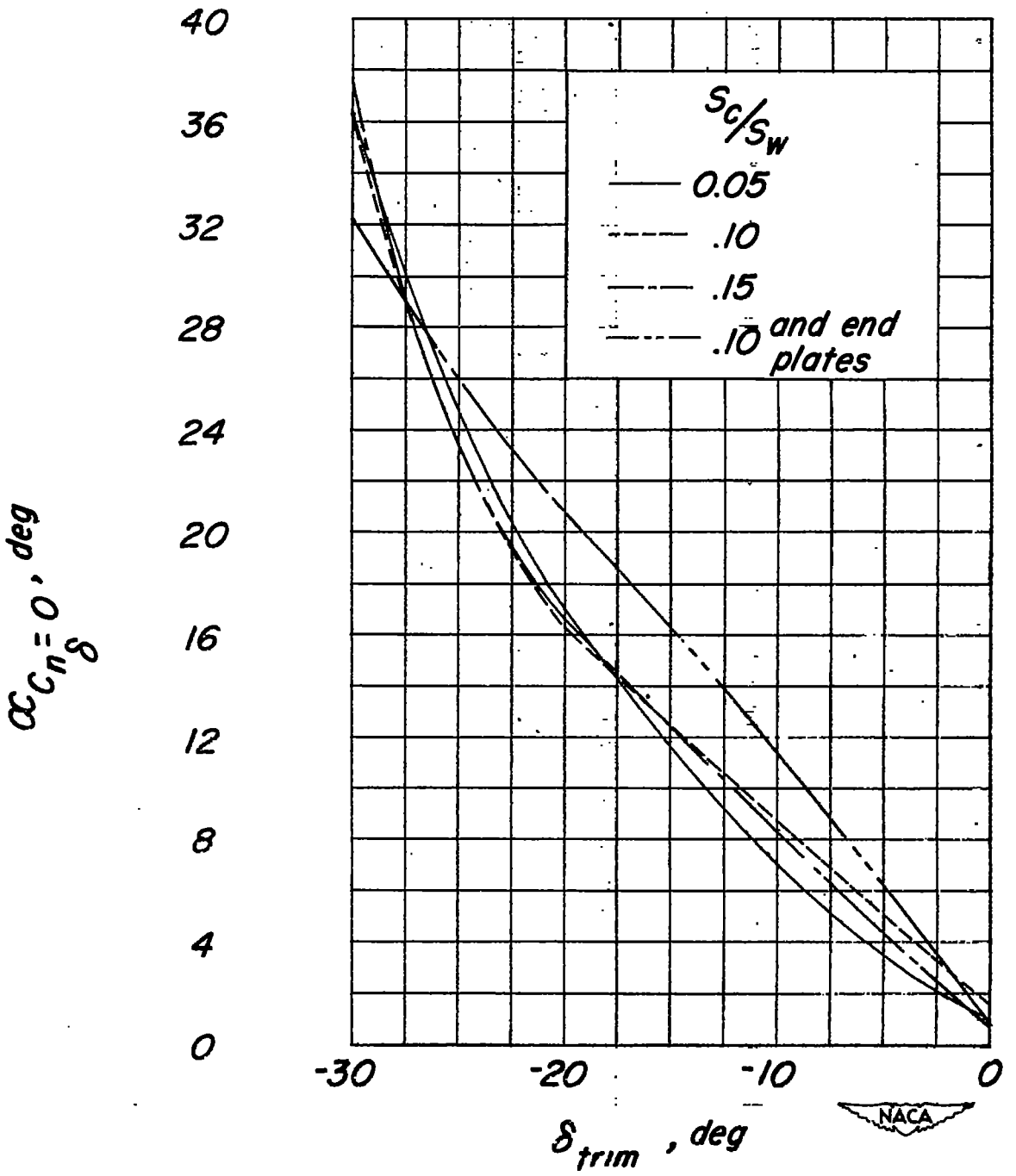

Figure 13.- Variation of the angle of attack for zero yawing moment with δ_{trim} for a 60° triangular-wing model having half-delta tip controls.

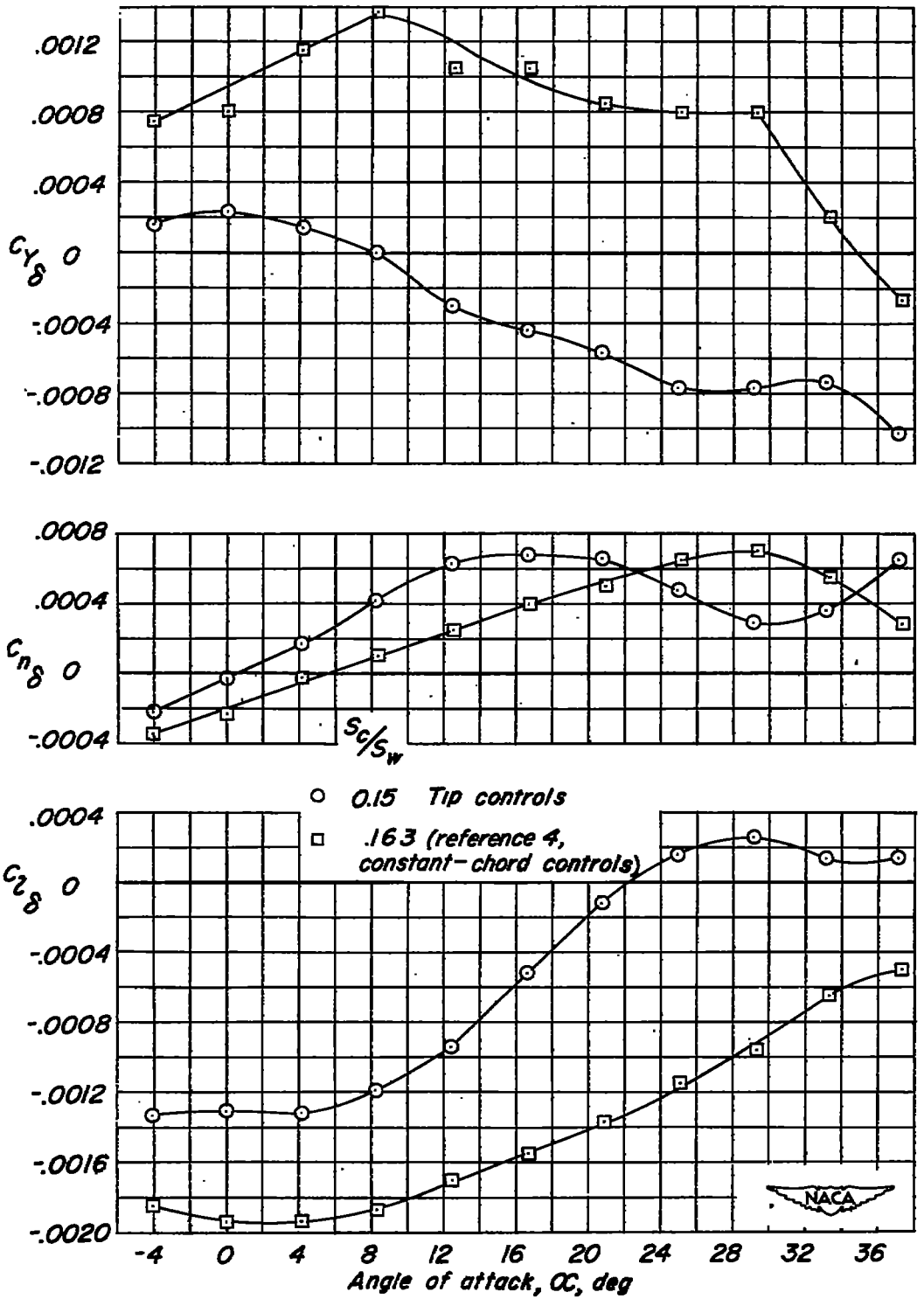

Figure 14.- Comparison of control parameters of a 60° triangular-wing model having half-delta tip controls or constant-chord controls. $\delta_{trim} = 0°$.

[redacted]

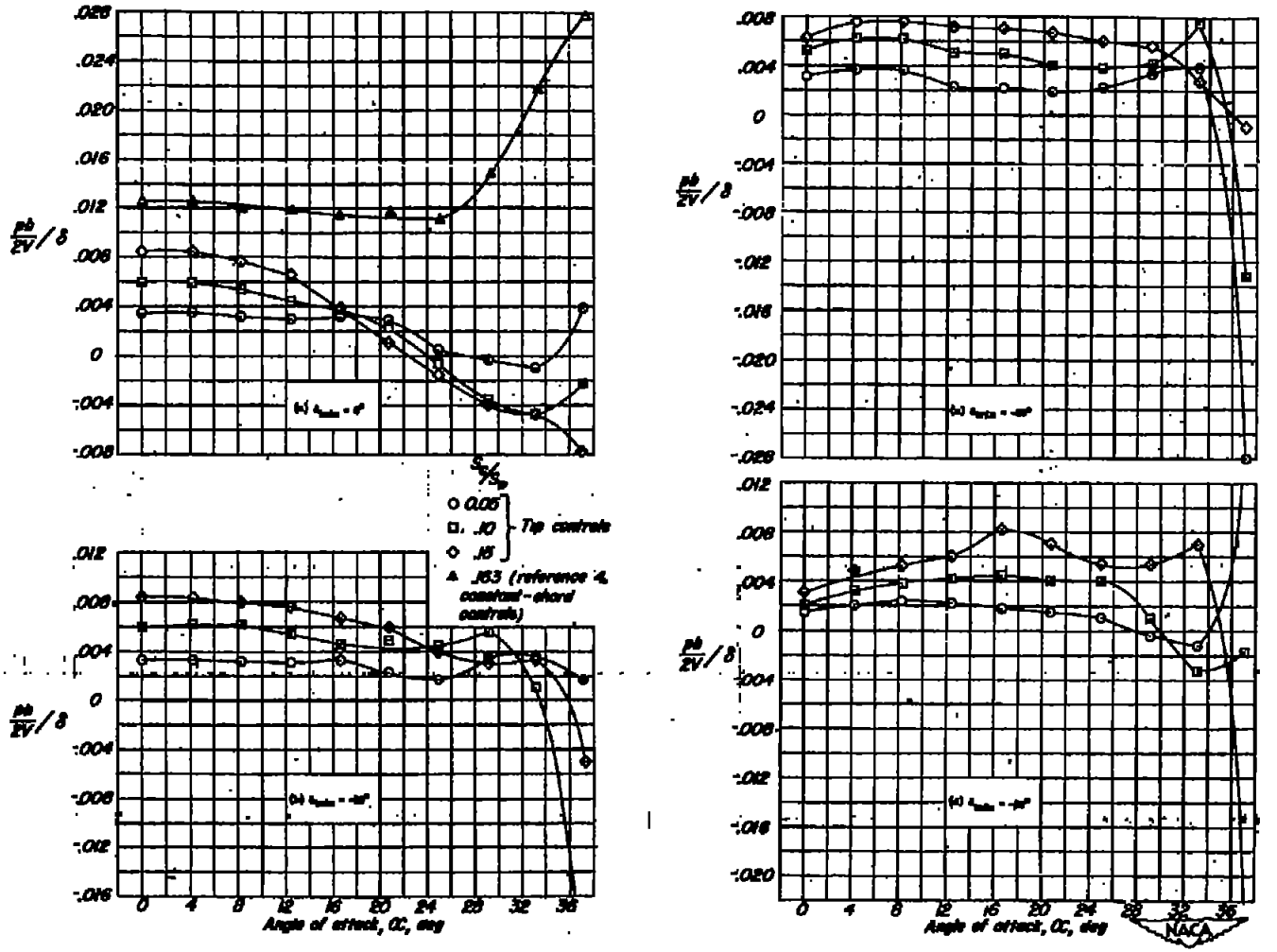

Figure 15.- Variation of $\frac{pb/2V}{\delta}$ with angle of attack for a 60° triangular-wing model having tip controls or constant-chord controls.

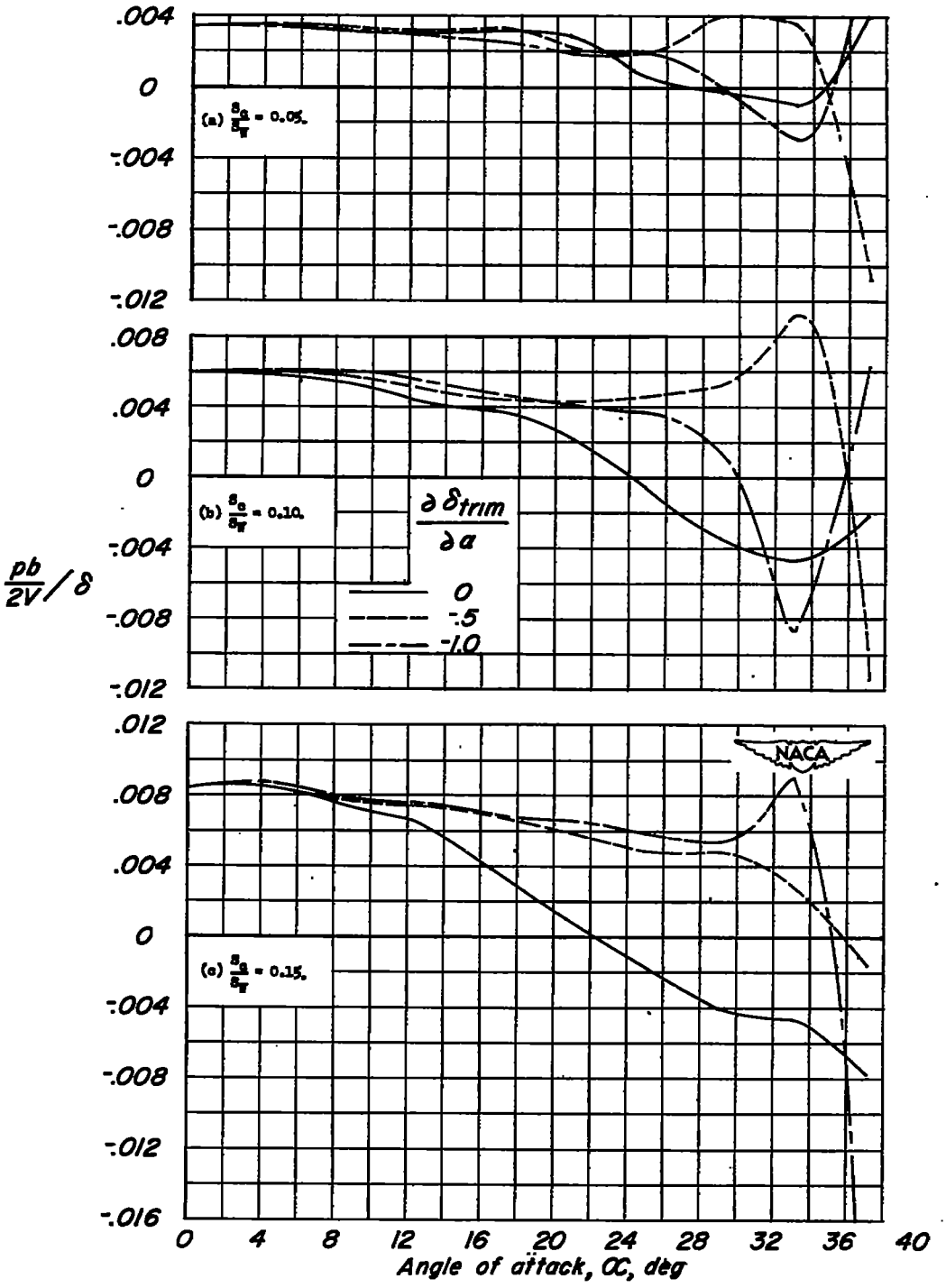

Figure 16.- Variation of $\frac{pb/2V}{\delta}$ with angle of attack for several values of $\frac{\partial \delta_{trim}}{\partial \alpha}$.

[redacted]

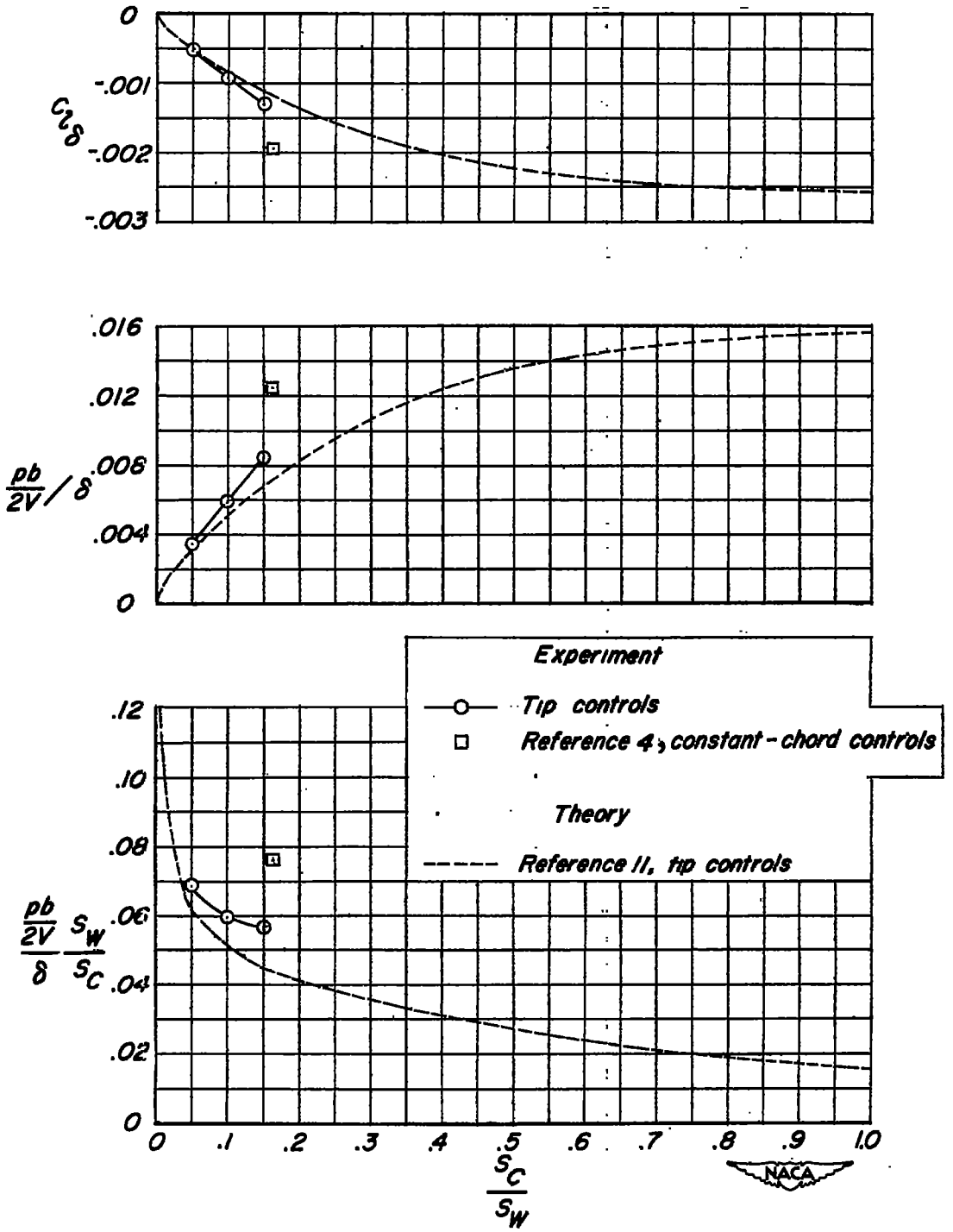

Figure 17.- Variation of C_{l_δ}, $\frac{pb/2V}{\delta}$, and $\frac{pb/2V}{\delta}\frac{S_w}{S_c}$ with S_c/S_w. Wing-fuselage combination; $\alpha = 0^\circ$; $\delta_{trim} = 0^\circ$.

[redacted]